(12) INTERNATIONAL APPLICATION PUBLISHED UNDER THE PATENT COOPERATION TREATY (PCT)

(19) World Intellectual Property Organization
International Bureau

(43) International Publication Date
3 January 2003 (03.01.2003)

PCT

(10) International Publication Number
WO 03/000125 A1

(51) International Patent Classification[7]: A61B 5/00, G06F 17/00

(21) International Application Number: PCT/GB02/02843

(22) International Filing Date: 21 June 2002 (21.06.2002)

(25) Filing Language: English

(26) Publication Language: English

(30) Priority Data:
0115284.2 22 June 2001 (22.06.2001) GB
0206382.4 19 March 2002 (19.03.2002) GB

(71) Applicant *(for all designated States except US)*: **CARDIODIGITAL LIMITED** [GB/GB]; 18 Blantyre Terrace, Edinburgh EH10 5AE (GB).

(72) Inventors; and
(75) Inventors/Applicants *(for US only)*: **ADDISON, Paul, Stanley** [GB/GB]; 58 Buckstone Crook, Edinburgh EH10 6UR (GB). **WATSON, James, Nicholas** [GB/GB]; 116 Lochview Drive, Hogganfield, Glasgow G33 1QF (GB).

(74) Agent: **MURGITROYD & COMPANY**; Scotland House, 165-169 Scotland Street, Glasgow G5 8PL (GB).

(81) Designated States *(national)*: AE, AG, AL, AM, AT, AU, AZ, BA, BB, BG, BR, BY, BZ, CA, CH, CN, CO, CR, CU, CZ, DE, DK, DM, DZ, EC, EE, ES, FI, GB, GD, GE, GH, GM, HR, HU, ID, IL, IN, IS, JP, KE, KG, KP, KR, KZ, LC, LK, LR, LS, LT, LU, LV, MA, MD, MG, MK, MN, MW, MX, MZ, NO, NZ, OM, PH, PL, PT, RO, RU, SD, SE, SG, SI, SK, SL, TJ, TM, TN, TR, TT, TZ, UA, UG, US, UZ, VN, YU, ZA, ZM, ZW.

(84) Designated States *(regional)*: ARIPO patent (GH, GM, KE, LS, MW, MZ, SD, SL, SZ, TZ, UG, ZM, ZW), Eurasian patent (AM, AZ, BY, KG, KZ, MD, RU, TJ, TM), European patent (AT, BE, CH, CY, DE, DK, ES, FI, FR, GB, GR, IE, IT, LU, MC, NL, PT, SE, TR), OAPI patent (BF, BJ, CF, CG, CI, CM, GA, GN, GQ, GW, ML, MR, NE, SN, TD, TG).

Published:
— *with international search report*

[Continued on next page]

(54) Title: WAVELET-BASED ANALYSIS OF PULSE OXIMETRY SIGNALS

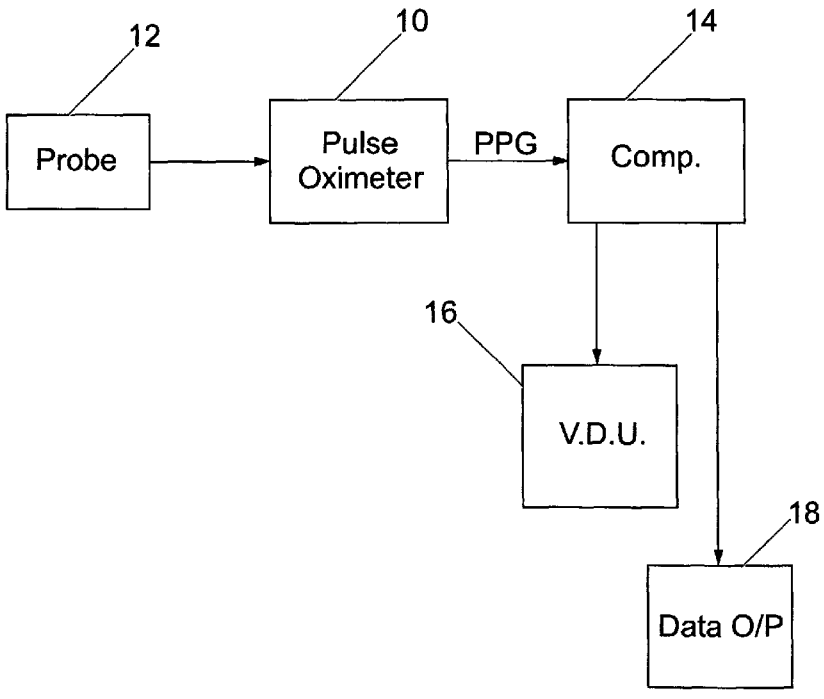

(57) Abstract: A pulse oximetry signal, suitably a photoplethysmogram (PPG), is decomposed by wavelet transform techniques, and the decomposed signal analysed to provide selected physiological data. The signal may be processed to remove noise, artefacts, or transient features. Information on respiration may also be recovered.

WO 03/000125 A1

— *before the expiration of the time limit for amending the claims and to be republished in the event of receipt of amendments*

For two-letter codes and other abbreviations, refer to the "Guidance Notes on Codes and Abbreviations" appearing at the beginning of each regular issue of the PCT Gazette.

'Wavelet-Based Analysis of Pulse Oximetry Signals'

Field of Invention

The present invention relates to a method of analysis of medical signals, and in particular to a method of decomposition of signals used in pulse oximetry. Specifically the invention relates to an improved method of denoising such signals and in the extraction of clinically useful information from such signals including the monitoring and analysis of patient respiration.

Background

Oximetry is an optical method for measuring oxygenated haemoglobin in blood. Oximetry is based on the ability of different forms of haemoglobin to absorb light of different wavelengths. Oxygenated haemoglobin (HbO_2) absorbs light in the red spectrum and deoxygenated or reduced haemoglobin (RHb)

absorbs light in the near-infrared spectrum. When red and infrared light is passed through a blood vessel the transmission of each wavelength is inversely proportional to the concentration of HbO_2 and RHb in the blood.

Pulse oximeters can differentiate the alternating light input from arterial pulsing from the constant level contribution of the veins and other non-pulsatile elements. Only the alternating light input is selected for analysis. Pulse oximetry has been shown to be a highly accurate technique.

The contemporary pulse oximeter unit normally provides three outputs:

1. the arterial oxygen saturation
2. the heart rate
3. a fluctuating time series - the pulse oximeter trace or *plethysmographic waveform*

The normal pulse oximeter waveform - the photoplethysmogram (PPG) - bears a strong resemblance to an arterial pressure waveform complete with dichrotic notch. A schematic of a typical pulse oximeter trace from a finger probe is shown in Figure 1a. The repeating double humped (with a notch A in-between) nature of the waveform is evident in the plot. Often, the second hump disappears and a signal such as that in Figure 1b is obtained. This may indicate a clinical condition such as reduced arterial compliance. Often, for this

type of signal, there is a marked change in the gradient of the falling waveform (i.e. a kink) as indicated by the arrow B in the plot.

Figure 2 contains a plot of three simultaneously acquired signals acquired from a patient. These are: a finger pulse oximetry trace, an ear pulse oximetry trace and an ECG. These 10 second segments have been cut from a much longer signal. Note the significant drift associated with the pulse oximetry traces.

Summary of the Invention

The invention provides a method of measuring physiological parameters, as defined in claim 1, and also provides a method of processing a pulse oximetry signal, as defined in claim 2.

From another aspect, the invention provides a physiological measurement system as defined in claim 22.

Preferred features and advantages of the invention will be apparent from the other claims and from the following description.

The invention in its preferred forms provides a method for the decomposition of pulse oximetry signals using wavelet transforms which allows for underlying characteristics which are of clinical use to be displayed and measured. The method utilises wavelet transforms to decompose the signal in

wavelet space. The wavelet decomposition of one or more or a combination of signals can then be used to:

(a) construct a wavelet visualisation of the signal - the preferred method being that which uses wavelet energy surfaces plotted against the location parameter *b* and the inverse of the dilation parameter *a*. This visualisation would highlight salient information in a more useful form for clinical diagnosis (e.g. see 2D and 3D scalograms in figures described below). This form of information presentation should facilitate the interpretation of such signals. It is envisaged that the clinician would be provided with a real time display of the scalogram.

(b) provide, through the position and amplitude of features in the scalogram, measurable characteristics of the signal for estimation of the health of the monitored patient. These characteristics may include wavelet-based parameters, including ratios, for the determination of oxygen saturation. This is important for the determination of the correct therapy for the patient.

(c) provide, using information derived from the wavelet transform (i.e. from the transform, scalogram (energy density) normalised scalogram, wavelet power spectrum, modulus maxima, wavelet ridges, phase representation, etc.) a method for measuring the cardiovascular system compliance.

(d) provide, using information derived from the wavelet transform (i.e. from the transform, scalogram (energy density) normalised scalogram, wavelet power spectrum, modulus maxima, wavelet ridges, phase representation, etc.) a method for detecting the presence and location of pertinent features (e.g. maxima, minima, notch, kink, etc.) and timescales within the pulse oximetry signal and use of this information for a clinically useful purpose.

(e) provide, using information derived from the wavelet transform (i.e. from the transform, scalogram (energy density) normalised scalogram, wavelet power spectrum, modulus maxima, wavelet ridges, phase representation, etc.) a method for identifying features of the wavelet power spectrum which can be used as clinical markers of the health of the patient at the time of data collection

(f) provide, using information derived from the wavelet transform (i.e. from the transform, scalogram (energy density) normalised scalogram, wavelet power spectrum, modulus maxima, wavelet ridges, phase representation, etc.) a method for identifying features which can be used as clinical markers of the future health of the patient, that is as markers of the subsequent deterioration or improvement of the health of the patient. These markers will be incorporated within a prediction algorithm.

(g) provide, using information derived from the wavelet transform (i.e. from the transform, scalogram (energy density) normalised scalogram, wavelet power spectrum, modulus maxima, wavelet ridges, phase representation, etc.) a method for detecting and monitoring the patient breathing signal. This method would be suitable for the monitoring the regularity of the breathing pattern and patient breathing rate where high levels of noise and erroneous artefact affects the signal. This information to be used in conjunction with other relevant clinical information for clinically useful purposes.

(h) provide, using information derived from the wavelet transform (i.e. from the transform, scalogram (energy density) normalised scalogram, wavelet power spectrum, modulus maxima, wavelet ridges, phase representation, etc.) an accurate method for detecting and monitoring the patient breathing rate. This information to be displayed on the pulse oximeter device. This information to be used in conjunction with other relevant clinical information for clinically useful purposes.

(i) provide a method for the disassociation of artefact from the pertinent signal components, where artefact includes noise, coherent signal, movement artefact and if required breathing artefact. The preferred method of performing this would be a modulus maxima technique.

(j) provide a method for the classification of the current status of the patient's health based on the wavelet transform features and incorporating a suitable classification method. The optimal combination of features will be employed. The classification methods may include non-parametric Bayesian classification methods, neural networks, etc. and also include preprocessing discriminant analysis techniques such as principle component analysis and/or linear discriminant analysis for reducing the dimensionality of multidimensional data.

(k) provide a method for the prediction of the future status of the patient's health based on the wavelet transform features and incorporating a suitable classification method. The optimal combination of features will be employed. The classification methods may include non-parametric Bayesian classification methods, neural networks, etc. and also include preprocessing discriminant analysis techniques such as principle component analysis and/or linear discriminant analysis for reducing the dimensionality of multidimensional data.

Embodiments of the invention will now be described, by way of example only, with reference to the drawings:

Figure 1(a): Arterial Pulse and Pulse Oximetry Signal, as discussed above.

Figure 1(b) Arterial Pulse and Pulse Oximetry Signal, as discussed above.

Figure 2: The Three Collected traces: Top - Ear pulse oximetry signal, Middle - Finger pulse oximetry signal, Lower - ECG.

Figure 3(a): Wavelet analysis of a 2 second segment of pulse oximetry signal taken from the ear 10 minutes into the recording. Top: the pulse oximetry trace. Bottom: the scalogram. Standard Morlet wavelet with ω_0=5.5

Figure 3(b): Wavelet analysis of a 2 second segment of pulse oximetry signal taken from the ear 10 minutes into the recording. The Phase plot. Standard Morlet wavelet with ω_0=5.5

Figure 3(c): Wavelet analysis of a 2 second segment of pulse oximetry signal taken from the ear 10 minutes into the recording. Top: the modulus maxima plot. Bottom: the ridge plot. Standard Morlet wavelet with ω_0=5.5

Figure 3(d): Wavelet analysis of a 2 second segment of pulse oximetry signal taken from the ear 10 minutes into the recording. Top: the pulse oximetry trace. Bottom: the scalogram. Complete Morlet wavelet with ω_0=3

Figure 3(e): Wavelet analysis of a 2 second segment of pulse oximetry signal taken from the ear 10

minutes into the recording. The Phase plot. Complete Morlet wavelet with ω_0=3

Figure 3(f): Wavelet analysis of a 2 second segment of pulse oximetry signal taken from the ear 10 minutes into the recording. Top: the modulus maxima plot. Bottom: the ridge plot. Complete Morlet wavelet with ω_0=3

Figure 4(a): Wavelet analysis of a 2 second segment of pulse oximetry signal taken from the finger 10 minutes into the recording. Top: the pulse oximetry trace. Bottom: the scalogram. Standard Morlet wavelet with ω_0=5.5

Figure 4(b): Wavelet analysis of a 2 second segment of pulse oximetry signal taken from the finger 10 minutes into the recording. The Phase plot. Standard Morlet wavelet with ω_0=5.5

Figure 4(c): Wavelet analysis of a 2 second segment of pulse oximetry signal taken from the finger 10 minutes into the recording. Top: the modulus maxima plot. Bottom: the ridge plot. Standard Morlet wavelet with ω_0=5.5

Figure 4(d): Wavelet analysis of a 2 second segment of pulse oximetry signal taken from the finger 10 minutes into the recording. Top: the pulse oximetry trace. Bottom: the scalogram. Complete Morlet wavelet with ω_0=3

Figure 4(e): Wavelet analysis of a 2 second segment of pulse oximetry signal taken from the finger 10 minutes into the recording. The Phase plot. Complete Morlet wavelet with ω_0=3

Figure 4(f): Wavelet analysis of a 2 second segment of pulse oximetry signal taken from the finger 10 minutes into the recording. Top: the modulus maxima plot. Bottom: the ridge plot. Complete Morlet wavelet with ω_0=3

Figure 5: Region Segmentation in Phase Space

Figure 6(a): Wavelet Denoising and Detrending. Morlet Wavelet ω_0=5.5. Original Signal.

Figure 6(b): Wavelet Denoising and Detrending. Morlet Wavelet ω_0=5.5. Scalogram

Figure 6(c): Wavelet Denoising and Detrending. Morlet Wavelet ω_0=5.5. Phase Plot

Figure 6(d): Wavelet Denoising and Detrending. Morlet Wavelet ω_0=5.5. Cropped Scalogram

Figure 6(e): Wavelet Denoising and Detrending. Morlet Wavelet ω_0=5.5. The original trace (top); the reconstructed trace (middle); the denoised and detrended trace (bottom).

Figure 7(a): Wavelet Denoising and Detrending. Morlet Wavelet ω_0=2. Original Signal.

Figure 7(b): Wavelet Denoising and Detrending. Morlet Wavelet ω_0=2. Phase Plot

Figure 7(c): Wavelet Denoising and Detrending. Morlet Wavelet ω_0=2. Original and reconstructed signals

Figure 7(d): Wavelet Denoising and Detrending. Morlet Wavelet ω_0=2. Blow up of Figure 7(c)

Figure 7(e): Wavelet Denoising and Detrending. Morlet Wavelet ω_0=2. Three different high frequency cut-off thresholds - increasing from top to bottom.

Figure 8(a): Scalogram showing the breathing ridge

Figure 8(b): A Collapsed Scalogram showing the breathing and heart rates.

Figure 9(a): The Analysis of a Plethysmogram Breathing Experiment Sub-Study:Pulse oximeter trace.

Figure 9(b): The Analysis of a Plethysmogram Breathing Experiment Sub-Study: The Modulus of the trace in Figure 9(a) showing ridges associated with pulse and breathing.

Figure 9(c): The Analysis of a Plethysmogram Breathing Experiment Sub-Study: the phase associated with the breathing ridges in Figure 9(b).

Figure 10(a): Phase following of respiration

Figure 10(b): Showing the steps of constant phase minima across scales.

Figure 11(a): Frequency Modulation of the dominant cardiac frequency bands

Figure 11(b): Amplitude Modulation of the dominant cardiac frequency bands

Figure 11(c): Individual Breathing features resolved using a low oscillation wavelet (One such feature indicated by arrow.)

Figure 12: A schematic diagram of the signal, its transformation as a scalogram, the associated wavelet power spectrum.

Figure 13: Partitioning of the test data. Power is plotted against entropy at the frequency levels given. An arbitrary separation line has been plotted (dashed) in the plot.

Figure 14(a): Graphical illustration of Bayesian Classification of 'ill' and 'healthy' data sets.

Figure 14(b): Graphical illustration of Bayesian Classification of 'ill' and 'healthy' data sets

Figure 15: Top: PPG signal. Lower Plot: The wavelet transform modulus maxima plot corresponding to the signal.

Figure 16: Top: A raw PPG signal. Lower Plot: The wavelet transform (threshold) filtered trace with individually isolated freatures of the trace marked by vertical lines.

Figure 17: A block schematic of an exemplary system for implementing the method of the invention.

The Wavelet transform

Wavelet transforms allow a signal to be decomposed such that both the frequency characteristics and the location of particular features in a time series may be highlighted simultaneously. This overcomes the basic shortcoming of Fourier analysis, where the spectrum only contains globally averaged information thus leading to location specific features in the signal being lost. The complete analysis of a signal requires the deduction of both the frequency make up and temporal location of the signal components. The limitation of Fourier (spectral-only) methods can be partly overcome by introducing a sliding time window which localises the analysis in time. This local or Short Time Fourier Transform (STFT) provides a degree of temporal resolution by highlighting

changes in spectral response with respect to time. However, this method is always a compromise between temporal and frequency resolution (higher frequency resolution means lower temporal resolution, and vice versa) due to the fixed window width associated with it. The nature of the wavelet transform is such that it is well suited to the analysis of signals in which a more precise time resolution is required for higher frequencies than for lower ones. By employing a variable width window, it effectively zooms in on the temporal signal when analysing higher frequencies, providing higher resolution where necessary.

The wavelet transform of a continuous real-valued time signal, $x(t)$, with respect to the wavelet function, ψ, is defined as

$$T(a,b) = \frac{1}{\sqrt{a}} \int_{-\infty}^{\infty} \psi^* \left(\frac{t-b}{a} \right) x(t) dt \qquad (1)$$

where t is time, a is the dilation parameter, b is the location parameter, $\psi^*((t-b)/a)$ is the complex conjugate of the analysing wavelet used in the convolution and $x(t)$ is the signal under investigation which, in this application, is the PPG signal obtained from the pulse oximeter. The wavelet transform can therefore be thought of as the cross-correlation of the analysed signal with a wavelet function that has been translated by a value b and dilated by a factor a.

Contemporary literature suggests two methods of wavelet analysis using either *discrete* or *continuous* transforms. The *discrete* wavelet transform necessitates the use of orthonormal wavelets, and dilation levels are set in the form of integer powers of two. This provides a rapid method of signal decomposition, and guarantees energy conservation and exact signal reconstruction. However, the discrete transform is limited by loss of both time and frequency resolution due to the dyadic nature of the transform. Conversely, the *continuous* wavelet transform does provide high resolution. Thus, proper use of wavelet analysis demands identification of the correct wavelet and transform type for the given application. The inherent redundancy in the continuous wavelet method, although computationally more intensive, increases clarity in the transform space and allows for greater temporal resolution at high dilations. For this reason we prefer to employ a continuous wavelet transform in our method. Note that in practice a discretised approximation to the continuous wavelet transform integral may be employed based on the FFT algorithm where the wavelet convolution in (1) is performed as a product in Fourier space (via the convolution theorem) hence speeding up the computation.

Any wavelet function may be used in the analysis. In the examples given here we employ complex Morlet wavelets. We define the complete Morlet wavelet as

$$\psi(t) = \frac{1}{\sqrt[4]{\pi}}(e^{i\omega_o t} - e^{-\frac{\omega_o^2}{2}})e^{-\frac{t^2}{2}} \qquad (2)$$

where ω_o is the central frequency of the mother wavelet, t is time, i is the complex number $(-1)^{1/2}$. The second term in the brackets is known as the correction term, as it corrects for the non-zero mean of the complex sinusoid of the first term. In practice it becomes negligible for values of $\omega_o > 5$. Most investigators concentrate on wavelet transforms with ω_o in the range 5~6, where it can be performed without the correction term since it becomes very small. In this case, the Morlet wavelet becomes

$$\psi(t) = \frac{1}{\sqrt[4]{\pi}} e^{i\omega_o t} e^{-\frac{t^2}{2}} \qquad (3)$$

This truncated Morlet wavelet is invariably used in the literature and often referred to as simply the *Morlet wavelet*. Here we use the name, 'standard Morlet wavelet', for this simplified form of equation 3 and 'complete Morlet wavelet', for the complete form given by equation 2.

Modulus maxima and ridges correspond to loci of local maxima and minima in the wavelet transform. These are useful in detecting singularities and following instantaneous frequencies. A vast amount of information is contained within the continuous wavelet transform $T(a,b)$. This can be condensed

considerably by considering only local maxima and minima of the transform. Two definitions of these maxima are commonly used in wavelet analysis practice, these are:

1 - Wavelet *ridges*, defined as

$$\frac{d\left(\left|T(a,b)^2\right|/a\right)}{da}=0 \qquad (4)$$

which are used for the determination of instantaneous frequencies and amplitudes of signal components. Notice that this definition of a ridge uses the rescaled scalogram $|T(a,b)|^2/a$ as it leads to a simpler analytical solution relating the ridge to the instantaneous frequency when a standard Morlet wavelet is employed as the analysing wavelet.

2 - Wavelet *modulus maxima*, defined as

$$\frac{d\,|T(a,b)|^2}{db}=0 \qquad (5)$$

are used for locating and characterising singularities in the signal. (Note that equations 4 and 5 also include inflection points with zero gradient. These can be easily removed when implementing the modulus maxima method in practice.)

In the present invention described here we use modulus maxima and ridges as defined above, however, any reasonable definition of the loci of the maxima

and minima of the transform may be incorporated within the method.

Details of the Method

Figures 3 and 4 show some results from preliminary wavelet analysis undertaken on short segments of pulse oximeter traces. Figure 3 corresponds to an ear probe signal and Figure 4 to a finger probe signal.

The left hand column (Figures 3(a),3(b),3(c), 4(a),4(b),4(c)) in each figure corresponds to the analysis performed using the standard Morlet wavelet with ω_0=5.5 and the right hand column (Figures 3(d),3(e),3(f),4(d),4(e),4(f)) corresponds to the analysis performed using the complete Morlet wavelet with ω_0=3. These ω_0=3 wavelets are much better for the temporal isolation of signal features.

The scalograms in Figures 3(a),3(d),4(a) and 4(d) are plotted below the original signals. The ω_0=5.5 plots exhibit more compactness in frequency as evidenced by the thinner horizontal high energy band corresponding to the 'beat' frequency of the pulse oximeter signal. Also evident are regular dips corresponding to the kinks in the signal. The ω_0=3 plots exhibit more temporal compactness where the dominant band contains undulation peaks which correspond to the repeating temporal pattern of the signal.

The phase plots are given below the scalograms in Figures 3 and 4 and provide information on the local matching of the wavelet with the signal. All phase plots shown exhibit regular repeating structure. The ω_0=3 phase plot is considerably less cluttered than the ω_0=5.5 plot due to less oscillatory nature of the wavelet used.

The lower plots in Figures 3 and 4 show the modulus maxima (top) and ridges (bottom) associated with the wavelet transform. These provide information concerning the location of temporal features and the instantaneous frequency of the signal respectively. Both methods allow for pertinent information within the highly redundant continuous wavelet transform to be presented (and hence extracted) in a more compact form. This information can be used within advanced filtering and prediction algorithms.

Elements of the Signal in Wavelet Space

Figure 5 contains one of the phase plots in Figure 4 blown up and split into four distinct regions. At the very low frequency range (region B-L) there is no obvious local coherent matching of the wavelet with the signal (see below for more information concerning this region). At the next lower frequency range (region P_1) the phase plots exhibit a smooth repeating pattern corresponding to the regular pulsing of the signal. Above this range these undulations split into two, (region P_2) where the location of this new split corresponds to the marked

change in slope (the kink) occurring at the decreasing part of the pulse oximeter waveform (it would correspond to the location of the notch for a double humped waveform). At the highest frequencies (region N) the phase changes become more irregular in their occurrence and correspond to the smaller fluctuations in the signal (e.g. high frequency noise, high frequency movement artefact, etc.) The features within each region could be further partitioned using advanced filtering techniques, for example incorporating wavelet modulus maxima or wavelet ridge filtering technology.

Wavelet Detrending and Denoising and the Elucidation of Breathing Artefact

Figure 6a shows a 35 second segment of pulse oximeter waveform. There is obvious drift in the signal. The corresponding scalogram and phase plots are given in Figures 6b and 6c respectively for a Morlet decomposition with ω_0=5.5. Figures 6d and 6e illustrate a simple wavelet-based method for detrending and denoising the signal where the scalogram is essentially cropped, i.e. the high and low wavelet bandpass centre frequencies are set to zero. This removes both the very small and very large period fluctuations associated with noise and drift respectively. Figure 6e shows, from top to bottom, the original signal, the reconstructed signal using all the scalogram information (a check) and the denoised and detrended signal reconstructed from the cropped scalogram in Figure 6d. More

advanced detrending and denoising includes filtering methodologies based on the wavelet transform modulus maxima and ridges, including methods to follow the ridges and other wavelet based features pertaining to the pulse and breathing signals through time.

Figure 7 contains the decomposition of the same signal as that in Figure 6, this time using a complete Morlet wavelet with $\omega_0=2$. The improved temporal isolation of the pulse features is apparent in the wavelet space scalogram of Figure 7a. In addition, the phase plot of Figure 7b shows a regular period oscillation at around 0.4 Hz particularly well. This, 2.5 second, periodicity corresponds to the regular breathing pattern of the patient- denoted as region B in the figure. In fact, we have separated the B-L region that was indicated in Figure 5 into region B - breathing - and region L - other lower frequency signal components including drift. The denoising and detrending of the signal is carried out in the same way as in the previous figure to give the denoised and detrended signal shown in the lower plot of Figure 7c. Figure 7d shows a blow up of the first five seconds of the signals in Figure 7c. The smoothing of the signal is obvious in the lower plot. The choice of the upper frequency cut-off is critical in partitioning relevant signal artefacts from noise. Figure 7e shows three plots of the denoised and detrended signal where progressively higher cut-off thresholds have been used. This allows higher and higher frequency features back into the denoised signal.

More on the elucidation of breathing artefact

Four, wavelet-based, methodologies may be employed for the monitoring of respiration and the extraction of the breathing rate from a standard pulse oximeter trace or photoplethysmograph (PPG) trace. These methodologies may be used independently, for example within an algorithm, or collectively using a polling mechanism. They are given as:

1. High amplitude banding.

When the breathing artefact is particularly pronounced, the breathing rate can be identified as a strong band or ridge of high transform values in the low (<1Hz) frequency range. The arrow in Figure 8(a) indicates one such ridge. In one preferred embodiment, this band can be identified by collapsing the scalogram down into two dimensions, as shown in Figure 8(b). This is a wavelet based power spectrum: the summation of coefficients across scales factored by the reciprocal of the square of the scale value ($1/a^2$). The primary assumptions made in this methodology are: (1) the dominant features in the filtered trace are cardiac components and (2) the breathing rate is less than the heart rate. Alternative assumptions can also be employed according to the clinical situation, e.g. PPGs from neonates.

In another embodiment, the breathing ridge may be followed in wavelet space using standard ridge-following techniques. This allows sudden or short term changes in breathing rate to be identified and quantified in real time. Evidence for the applicability of this methodology is found in Figure 9. Here a pulse oximeter trace, Figure 9(a), is presented for a 60 second experiment. During the experiment the subject was instructed to half his breathing rate after 30 seconds. As can be seen in Figure 9(b), a breathing ridge is clearly identifiable. This ridge drops in frequency (right hand horizontal scale) after 30 seconds. By identifying the phase of the wavelet transform along the ridge a clear indication of the timing of each breath can be determined - see Figure 9(c).

2. Phase methods.

As shown above, the phase of the wavelet coefficients can be used to identify the timing of each breath. However, cross-scale correlation of phase values, particularly for scalograms of low oscillation wavelets, can also be used as an indicator for low frequency, low amplitude, breathing features within the PPG trace.

In Figure 10(a) a portion of the wavelet phase space scalogram is presented. As can be seen there is a very definite cross-scale correlation for the frequencies around the breathing rate - the dotted box (i.e. similar phase values are aligned

vertically). By plotting the number of near zero modulus minima of the phase per scale against scale one can identify these areas of alignment as constant valued steps in the graph.

In the example of Figure 10(b) the scale (horizontal) axis is presented as the band pass centre frequency of that scale. This diagram plots the count of phase modulus minima per scale against scale. This is indicative of the cross scale correlation in the wavelet phase space and can be used to associate regions of the scalogram with physiological features (e.g. breathing and heart rate). This diagram is the count of phase minima of the scalogram shown in Figure 8.

As one can clearly see in this figure, the steps of constant phase count correlate extremely well with the wavelet spectrum peak positions of Figure 8(b) (the spectrum of the same trace as that of Figure 10(b)).

Note that the use of cross-correlation across scale can also be used to isolate individual features within the trace. See, for example, Figure 16, where individual pulse features within the trace have been identified by finding the dominant frequency associated with the heart rate then following the points of equal phase up to higher frequencies. These techniques cannot be performed using conventional STFT methods where the temporal resolution at high frequencies is inferior and phase

values are relative to the STFT frame origin rather than the wavelet centre.

3. Frequency modulation.

In some cases the amplitudes of the breathing related features within the PPG are such that they cannot easily be isolated as independent features within the transform space (e.g. they are of small amplitude, close to the dominant cardiac signal, etc). However, their effects on the dominant cardiac features can be observed. This is shown in Figure 11(a) where the frequency of modulation corresponds to the breathing rate of the subject. Associated frequency of the cardiac features oscillate with a frequency identified as that of the breathing rate. This method cannot be utilised using standard Fourier techniques where temporal averaging reduces resolution in time so making identification of this modulation undetectable.

4. Amplitude modulation.

In some cases the amplitudes of the breathing related features within the PPG are such that they cannot easily be isolated as independent features within the transform space (e.g. they are of small amplitude, close to the dominant cardiac signal, etc). However, their effects on the dominant cardiac features can be observed. This is shown in Figure 11(b) where the frequency of amplitude modulation corresponds to the breathing rate of the subject.

The amplitude dominant band corresponding to the cardiac features in wavelet space oscillates with a frequency identified as that of the breathing rate. Occasionally, when breaths are well separated individual breath features can be identified instead of a continuous, or modulated, band. This is particularly apparent when a low oscillation wavelet function is employed, as in Figure 11(c). Again, this method cannot be utilised using standard Fourier techniques where temporal averaging reduces resolution in time so making identification of this modulation undetectable.

Wavelet Feature Analysis

A scheme is described for the analysis of features derived from statistical measures of the wavelet transformed signal at a given frequency level or by following a time-frequency feature in wavelet space - where the transform can be represented as the actual transform values, the modulus of transform values, the squared transform values (the scalogram) or some other simple transformation of the wavelet transform values. In the preferred embodiment these features derived from the wavelet transform at a selected frequency level may include the power, mean, skew, kurtosis and entropy. In addition, these may be found for the peak frequency for each individual scalogram rather than a constant predefined frequency level, where peak frequency is defined as the frequency level containing the most power when integrated across the scalogram to

produce a wavelet power spectrum. Figure 12 shows a schematic of the wavelet transform scalogram and the wavelet power spectrum obtained from integration along the time domain at each frequency level. The selected frequency level across which the statistical measures are obtained is shown dashed in the scalogram plot.

The algorithm allows the analysis of segments of the pulse oximetry signals. The algorithm also allows the visual inspection of the feature scatter in parameter space. The feature scatter is then used as input to a classification method e.g. a Bayesian classifier or neural network.

Figure 13 shows the scatter plot derived from a signal data set obtained from two groups of children. One of the groups comprised a number of 'controls' taken from healthy children and were of relatively short duration these are marked by a 'o' in the figure. The other group were acquired from admitted patients attending the accident and emergency department of a UK children's hospital. Trace segments were selected from a PPG signal from each child and then decomposed using a wavelet transform. The feature distribution within the resulting scalograms were then probed across levels. The graph in Figure 13 has been plotted with a logarithmic vertical axis to better separate the feature points in parameter space. This scaling is optional and linear scaling may better suit other chosen features. We can see from visual inspection

that the controls are well separated from the admitted patients. The dashed line in the plot has been added for illustration and represents a possible separation line for dividing the two-dimensional data set into two classes.

In order to determine from a data set which illness severity the patient belongs to a Bayesian or other classification method may be employed. Figure 14 shows an example of the Bayesian classifier for the 'ill' and 'healthy' entropy data sets which gives a specificity of 84% and sensitivity of 81% for the determination of an 'ill' patient from a data sample. Figure 14(a) shows smoothed data PDF's (Probability Density Functions) corresponding to the Entropy data given by the horizontal axis of Figure 13. In Figure 14(b) Top plot: smoothed PDF's, Second top plot: smoothed PDF's weighted according to class prevalence, Second bottom plot: probability of observation stemming from class 'healthy' or 'ill', Bottom plot: the classifier training towards a 95% sensitivity for detecting 'ill' patients.

Note that the two data sets have been smoothed prior to the classification. The classifier may be trained using an iterative procedure and a risk matrix to enhance the sensitivity (say to 95% or above) at the expense of sensitivity. For example, for 96% sensitivity, a specificity of only 43% is attained for the entropy data set produce (lowest plot of Figure 14b).

Combinations of feature vectors can produce enhanced specificity-sensitivity values but with the requirement of increased computational effort. Figure 13 contained a two-dimensional feature set (of power and entropy). The increased computational effort arising from the use of multidimensional feature sets can be remedied somewhat by reducing the number of components using, for example, principal component analysis or linear discriminant analysis during the preprocessing stage.

The use of features derived from wavelet transform are useful as clinical markers of current state of the patient health as shown in the example. The same classification method may also be used as a predictor of the future state of the patient's health by correlating future outcomes with wavelet feature data.

The classification method may also be extended to include other clinical parameters including triage category, capillary refill time, white cell count, age, etc.

The classification method may also be extended to further partition the data according to patient 'illness severity', where the system is initially trained on illness severities determined using suitable criteria by a clinician.

Usefulness in the Measurement of Compliance etc.

The wavelet-based denoising and feature extraction described herein will allow for a more accurate analysis of the photoplethysmographic waveform when used in the measurement and monitoring of physiological parameters. An example of this is in the determination of arterial compliance using the shape of, and reference points within, the plethysmographic signal. Modulus maxima following can be used to determine the location and nature of pertinent characteristic points in the PPG, e.g. the beginning and end of the initial upslope of the PPG trace, maxima, minima, etc. This is shown schematically in Figure 15. Example PPG reference points used in the determination of clinically useful parameters are shown A,B,C,D and can be identified in the modulus maxima plot. The maxima lines can be used to better identify the characteristic points from within the signal.

In Figure 16 the lower plot shows the wavelet transform (filtered) trace with individually isolated features of the trace marked by vertical lines. Note these have been identified through cross scale correlation of phase. Note also that peaks and troughs have been differentiated through the phase value - near zero corresponding to peaks and near $\pm\pi$ corresponding to troughs.

Implementation

Figure 17 illustrates schematically one system for implementing the method of the invention.

A pulse oximeter 10 of known type has a probe 12 for obtaining readings from the finger, ear lobe or other suitable part of a patient. The pulse oximeter outputs a raw PPG signal to a computer 14 which carries out the wavelet transforms and associated analysis as discussed above. The computer 14 can output both the raw PPG signal and the results of processing the PPG signal to a VDU 16 and/or provide an output in the form of data at 18. The data output 18 may be in the form of a link to a remote location, a data carrier such as a disc or tape, or any other suitable format.

The mathematics of wavelet transforms are well described in the literature and known to those of ordinary skill in the art, and are not further described herein.

The immediately convenient manner of implementing the present invention is by connecting a computer to an existing pulse oximeter, as shown in Figure 17. It will be readily apparent, however, that the invention could equally well be implemented by combining a pulse oximeter with suitable computational resources within a single, stand-alone instrument; or by passing the PPG signal from a conventional pulse oximeter over a data communications link to a remote computer which could be shared with other users.

CLAIMS

1. A method of measuring physiological parameters, comprising using a pulse oximeter to obtain a pulse oximetry signal, decomposing the pulse oximetry signal by wavelet transform analysis, and deriving one or more physiological parameters from the decomposed signal.

2. A method of processing a pulse oximetry signal, in which the pulse oximetry signal is decomposed by wavelet transform analysis.

3. A method according to claim 1 or claim 2, in which the pulse oximetry signal is a photoplethysmogram (PPG).

4. A method as claimed in any preceding claim, including the steps of deriving the wavelet energy surfaces of the pulse oximeter signal, and plotting the surfaces against a location parameter and a scale parameter.

5. A method as claimed in any preceding claim, including the steps of deriving the wavelet transform modulus of the pulse oximeter signal, and plotting the modulus against a location parameter and a scale parameter.

6. A method as claimed in claim 4 or claim 5, in which the scale parameter is a characteristic

frequency of the wavelet used in the decomposition.

7. A method as claimed in claim 4 or claim 5, in which the scale parameter is the wavelet dilation.

8. A method as claimed in any preceding claim, including visually displaying information derived from the pulse oximetry signal by the wavelet transform analysis.

9. A method as claimed in claim 8, in which said information is displayed in real time.

10. A method as claimed in claim 8 or claim 9, in which said information includes one or more of:

the distribution of energies within the pulse oximetry signal,

coherent structures in the processed signal,

a contour plot of the decomposed waveform,

a surface plot of the decomposed waveform, and

a 2D or 3D energy scalogram.

11. A method according to any of claims 8 to 10, in which the unprocessed pulse oximetry signal is also displayed.

12. A method according to any preceding claim, in which the processing of the pulse oximetry

signal is effective to derive information relating to respiration.

13. A method according to claim 12, in which respiration information is derived from high amplitude ridges using ridge-following methods.

14. A method according to claim 12, in which the respiration information is derived by phase methods.

15. A method according to claim 14, in which the respiration information is derived by cross-scale correlation of phase values.

16. A method according to claim 12, in which the respiration information is derived by analysis of amplitude or frequency modulation.

17. A method according to any preceding claim, in which the processing of the pulse oximetry signal is effective to remove at least one of noise, artefact, and transient features.

18. A method according to claim 17, in which said removal employs inverse transformation of the cropped transform.

19. A method according to claim 17, in which said removal employs wavelet ridge methods.

20. A method according to claim 17, in which said removal employs modulus maxima methods.

21. A method according to any preceding claim, in which information from the transform is used to determine the present or predicted severity of illness of a subject.

22. A physiological measurement system comprising:

a pulse oximeter which includes an optical probe and circuit means connected to the probe to derive a pulse oximetry signal from a subject when the probe is applied to the subject, and

signal processing means arranged to receive the pulse oximetry signal and to process the signal by wavelet transform techniques.

22. A system according to claim 21, in which the signal processing means is arranged to process the pulse oximetry signal by the method of any of claims 3 to 21.

23. A system according to claim 21 or claim 22, further including a visual display unit operable to display the pulse oximetry signal and information derived therefrom in real time.

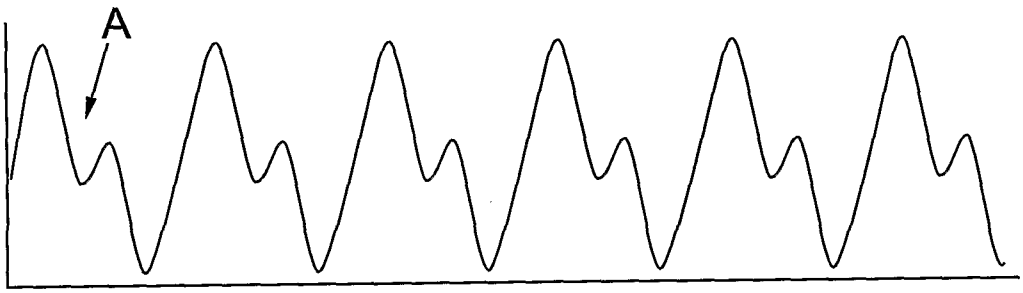

Fig. 1a

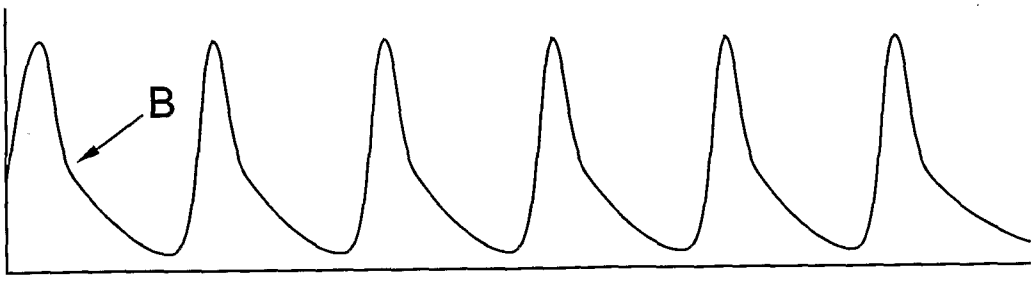

Fig. 1b

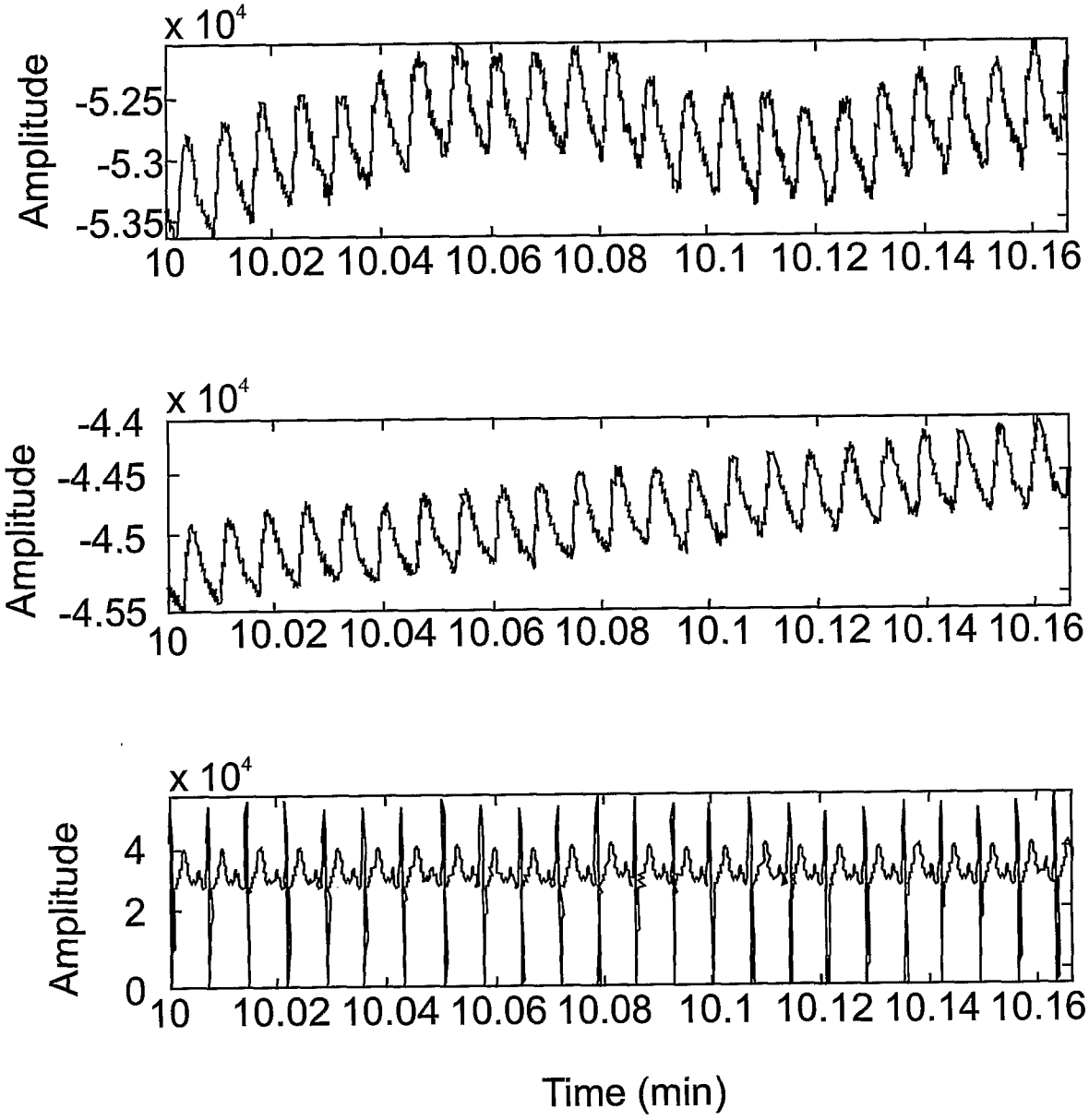
x 10^4
Amplitude
-5.25
-5.3
-5.35
10
10.02
10.04
10.06
10.08
10.1
10.12
10.14
10.16
x 10^4
Amplitude
-4.4
-4.45
-4.5
-4.55
10
10.02
10.04
10.06
10.08
10.1
10.12
10.14
10.16
x 10^4
Amplitude
4
2
0
10
10.02
10.04
10.06
10.08
10.1
10.12
10.14
10.16
Time (min)

Fig. 2

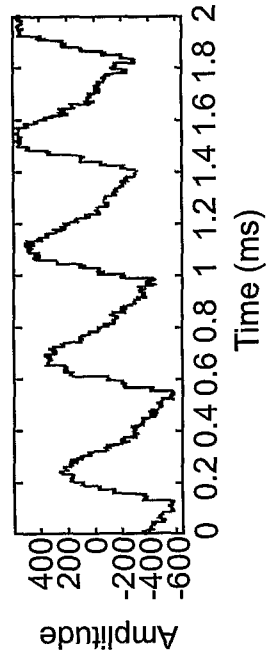
Amplitude
400
200
0
-200
-400
-600
0 0.2 0.4 0.6 0.8 1 1.2 1.4 1.6 1.8 2
Time (ms)

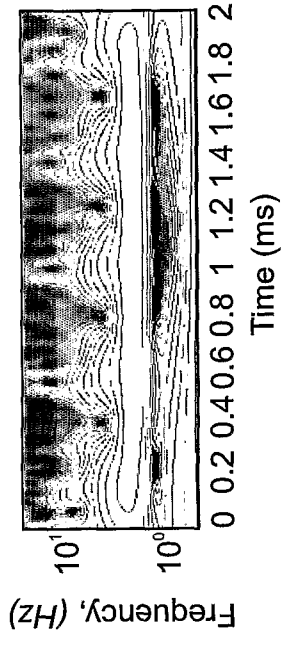
Frequency, (Hz)
10^1
10^0
0 0.2 0.4 0.6 0.8 1 1.2 1.4 1.6 1.8 2
Time (ms)

Fig. 3d

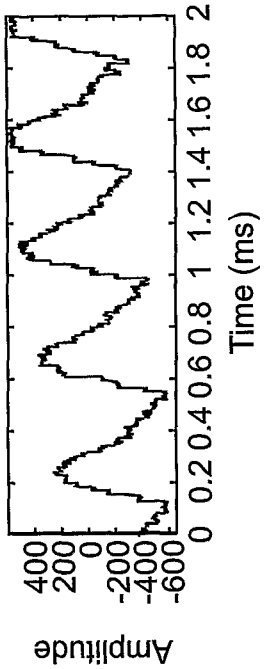
Amplitude
400
200
0
-200
-400
-600
0 0.2 0.4 0.6 0.8 1 1.2 1.4 1.6 1.8 2
Time (ms)

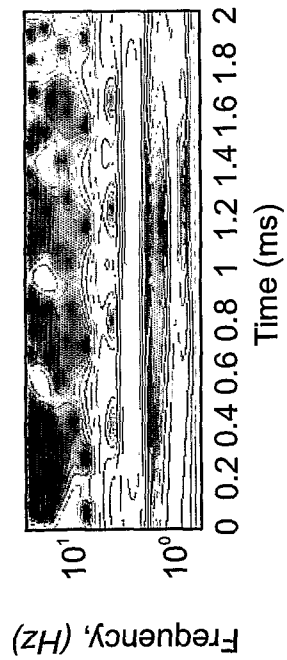
Frequency, (Hz)
10^1
10^0
0 0.2 0.4 0.6 0.8 1 1.2 1.4 1.6 1.8 2
Time (ms)

Fig. 3a

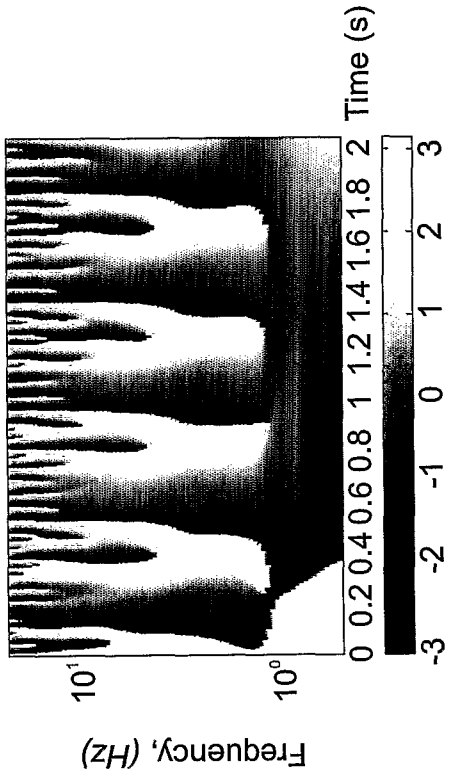
Time (s)
0 0.2 0.4 0.6 0.8 1 1.2 1.4 1.6 1.8 2
-3 -2 -1 0 1 2 3
10^1
10^0
Frequency, (Hz)

Fig. 3e

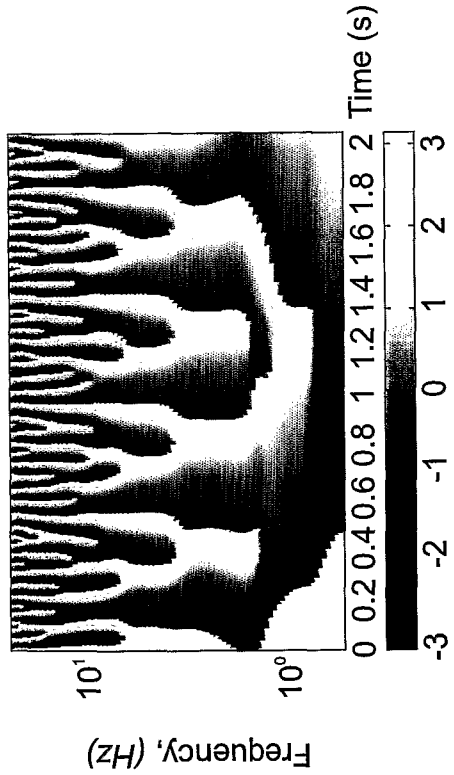
Time (s)
0 0.2 0.4 0.6 0.8 1 1.2 1.4 1.6 1.8 2
-3 -2 -1 0 1 2 3
10^1
10^0
Frequency, (Hz)

Fig. 3b

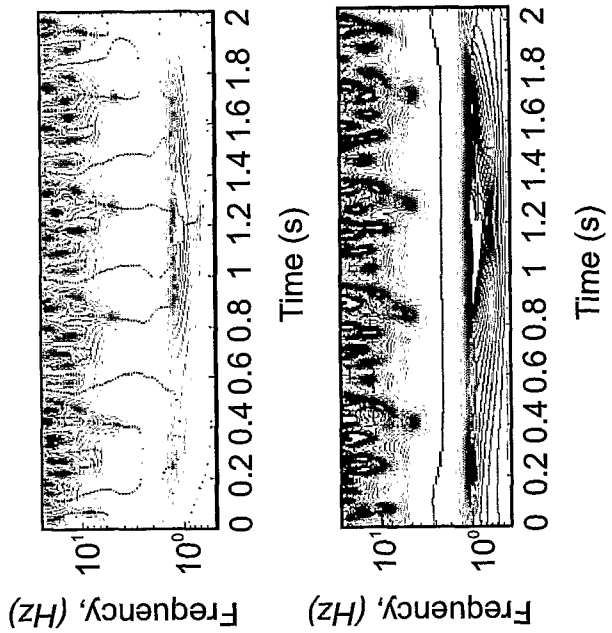
Frequency, (Hz)
Time (s)
0 0.2 0.4 0.6 0.8 1 1.2 1.4 1.6 1.8 2
10^1
10^0
Frequency, (Hz)
Time (s)
0 0.2 0.4 0.6 0.8 1 1.2 1.4 1.6 1.8 2
10^1
10^0

Fig. 3f

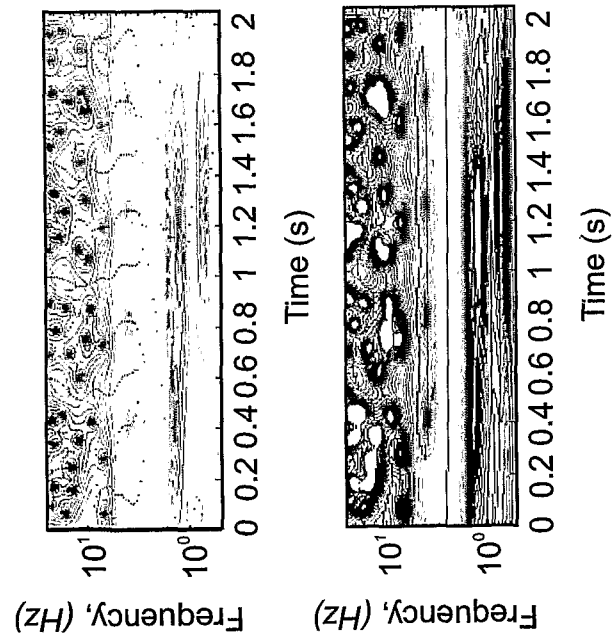
Frequency, (Hz)
Time (s)
0 0.2 0.4 0.6 0.8 1 1.2 1.4 1.6 1.8 2
10^1
10^0
Frequency, (Hz)
Time (s)
0 0.2 0.4 0.6 0.8 1 1.2 1.4 1.6 1.8 2
10^1
10^0

Fig. 3c

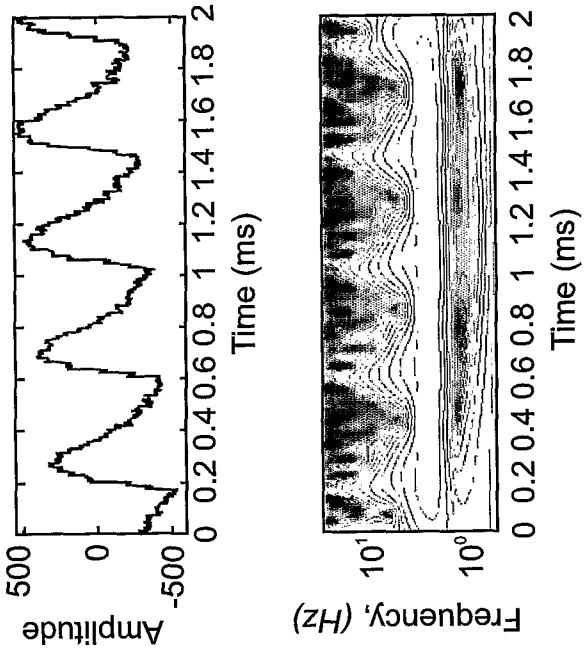
Amplitude
500
0
-500
0 0.2 0.4 0.6 0.8 1 1.2 1.4 1.6 1.8 2
Time (ms)
Frequency, (Hz)
10^1
10^0
0 0.2 0.4 0.6 0.8 1 1.2 1.4 1.6 1.8 2
Time (ms)

Fig. 4d

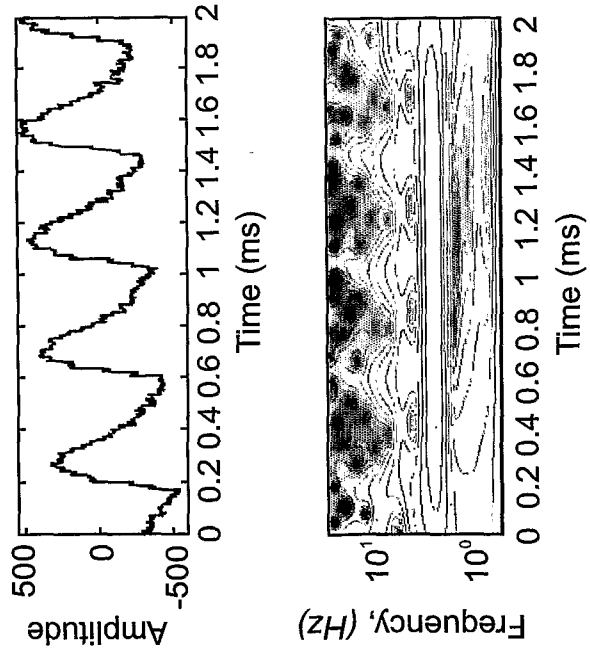
Amplitude
500
0
-500
0 0.2 0.4 0.6 0.8 1 1.2 1.4 1.6 1.8 2
Time (ms)
Frequency, (Hz)
10^1
10^0
0 0.2 0.4 0.6 0.8 1 1.2 1.4 1.6 1.8 2
Time (ms)

Fig. 4a

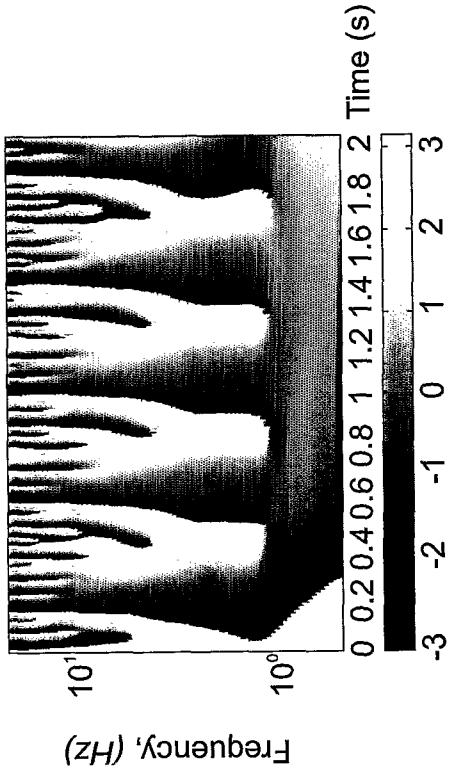
Time (s)
0 0.2 0.4 0.6 0.8 1 1.2 1.4 1.6 1.8 2
-3 -2 -1 0 1 2 3
10^1
10^0
Frequency, (Hz)

Fig. 4e

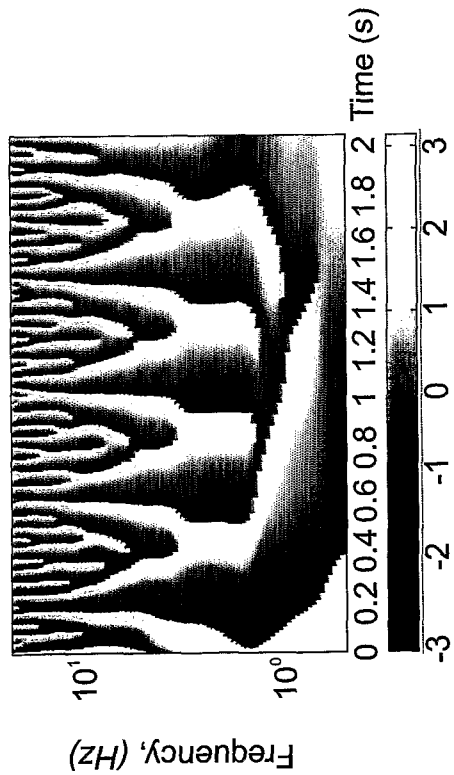
Time (s)
0 0.2 0.4 0.6 0.8 1 1.2 1.4 1.6 1.8 2
-3 -2 -1 0 1 2 3
10^1
10^0
Frequency, (Hz)

Fig. 4b

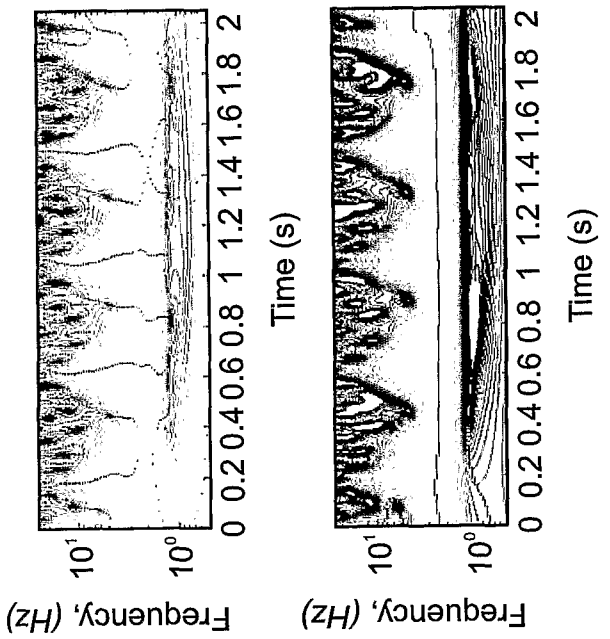
Frequency, (Hz)
10^1
10^0
0 0.2 0.4 0.6 0.8 1 1.2 1.4 1.6 1.8 2
Time (s)
Frequency, (Hz)
10^1
10^0
0 0.2 0.4 0.6 0.8 1 1.2 1.4 1.6 1.8 2
Time (s)

Fig. 4f

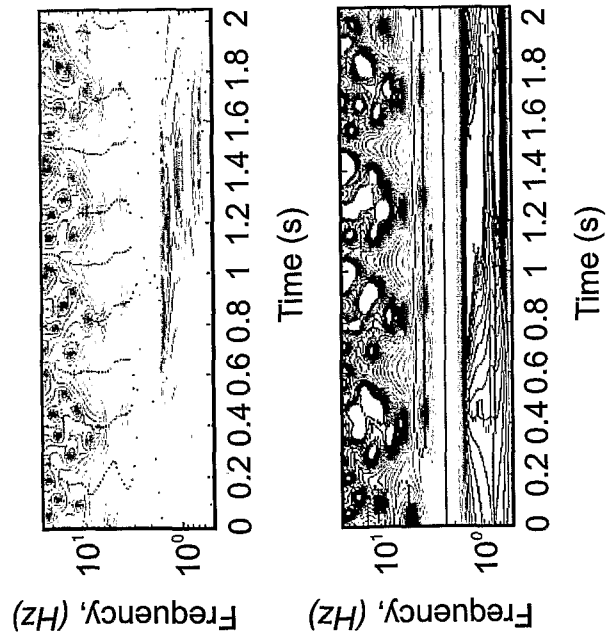
Frequency, (Hz)
10^1
10^0
0 0.2 0.4 0.6 0.8 1 1.2 1.4 1.6 1.8 2
Time (s)
Frequency, (Hz)
10^1
10^0
0 0.2 0.4 0.6 0.8 1 1.2 1.4 1.6 1.8 2
Time (s)

Fig. 4c

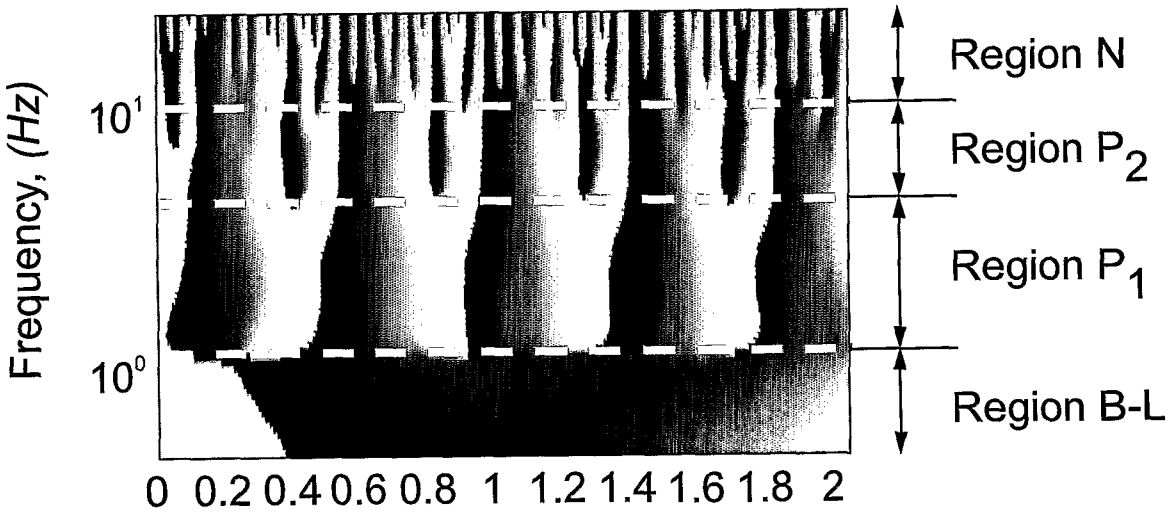
Frequency, (Hz)
10^1
10^0
0 0.2 0.4 0.6 0.8 1 1.2 1.4 1.6 1.8 2
Region N
Region P_2
Region P_1
Region B-L

Fig. 5

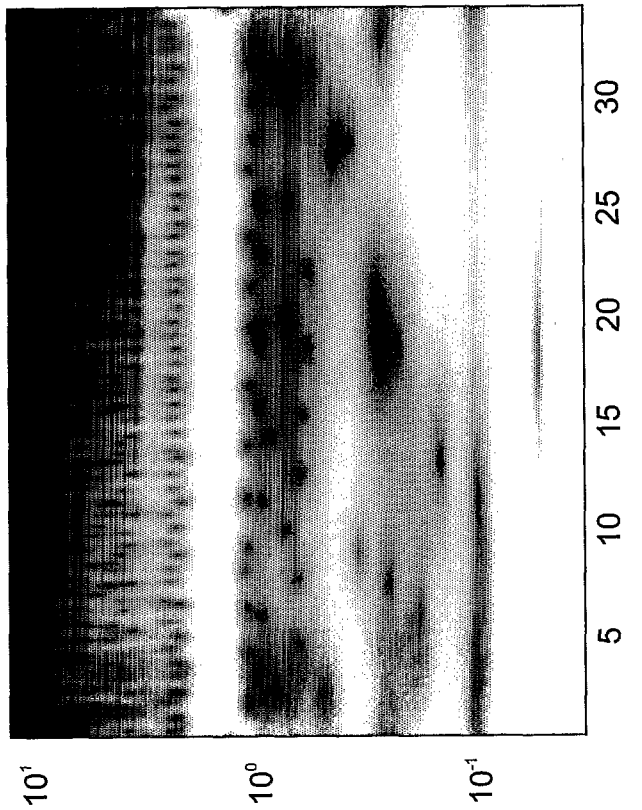
5
10
15
20
25
30
10^{1}
10^{0}
10^{-1}

Fig. 6b

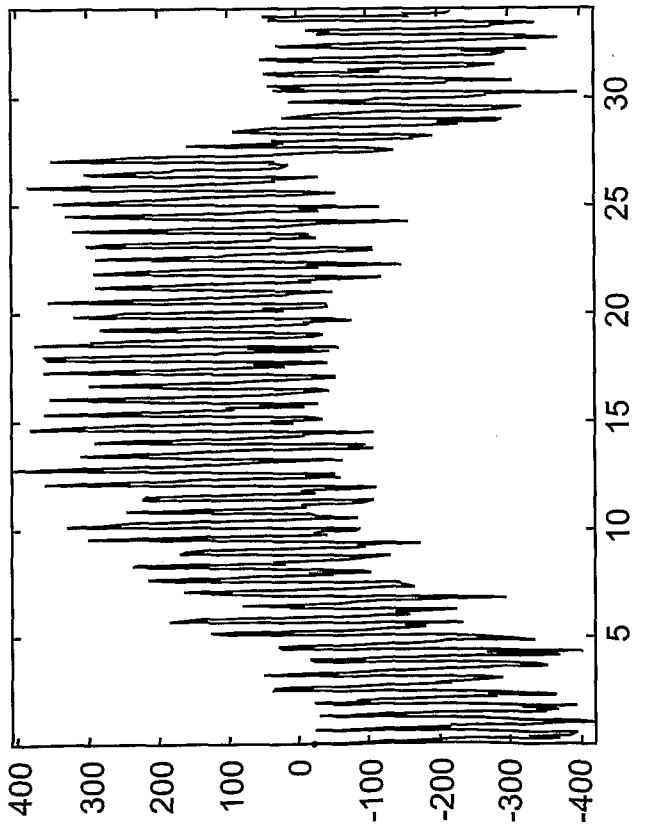
5
10
15
20
25
30
400
300
200
100
0
-100
-200
-300
-400

Fig. 6a

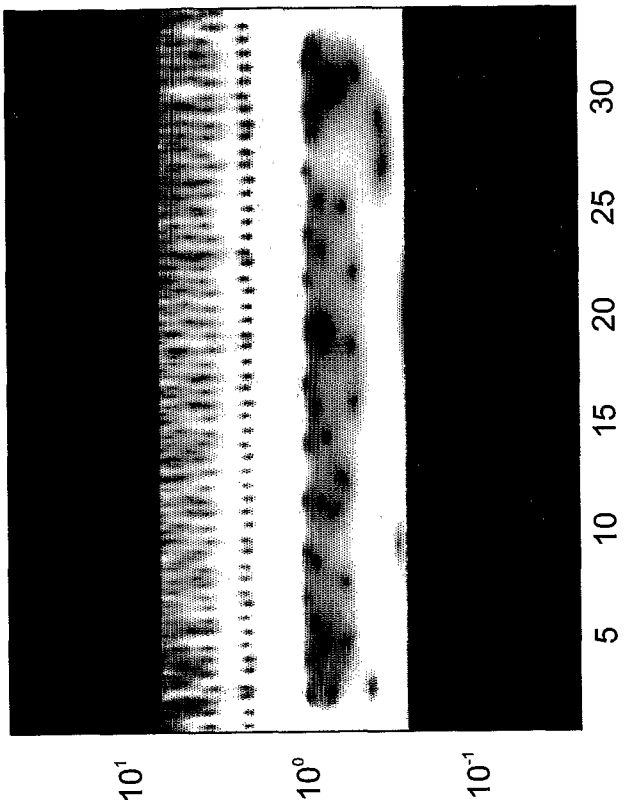

Fig. 6d

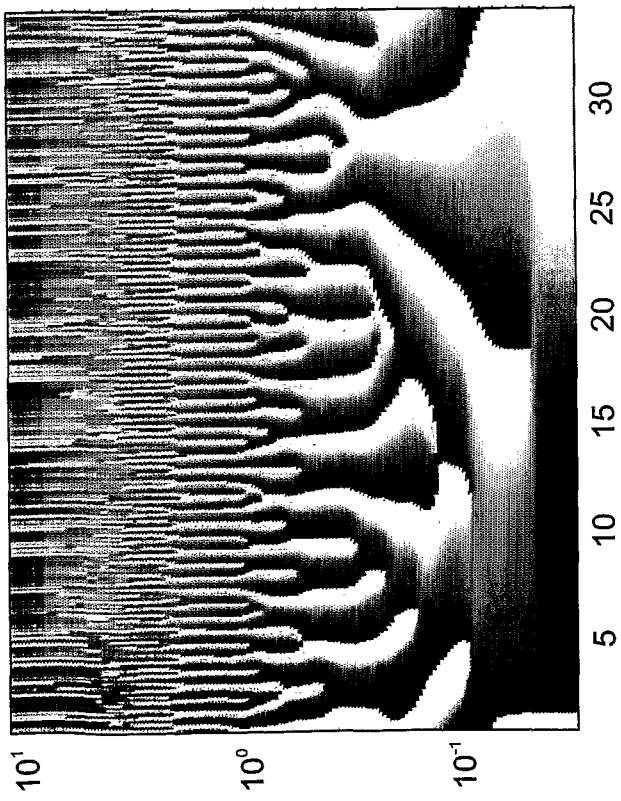

Fig. 6c

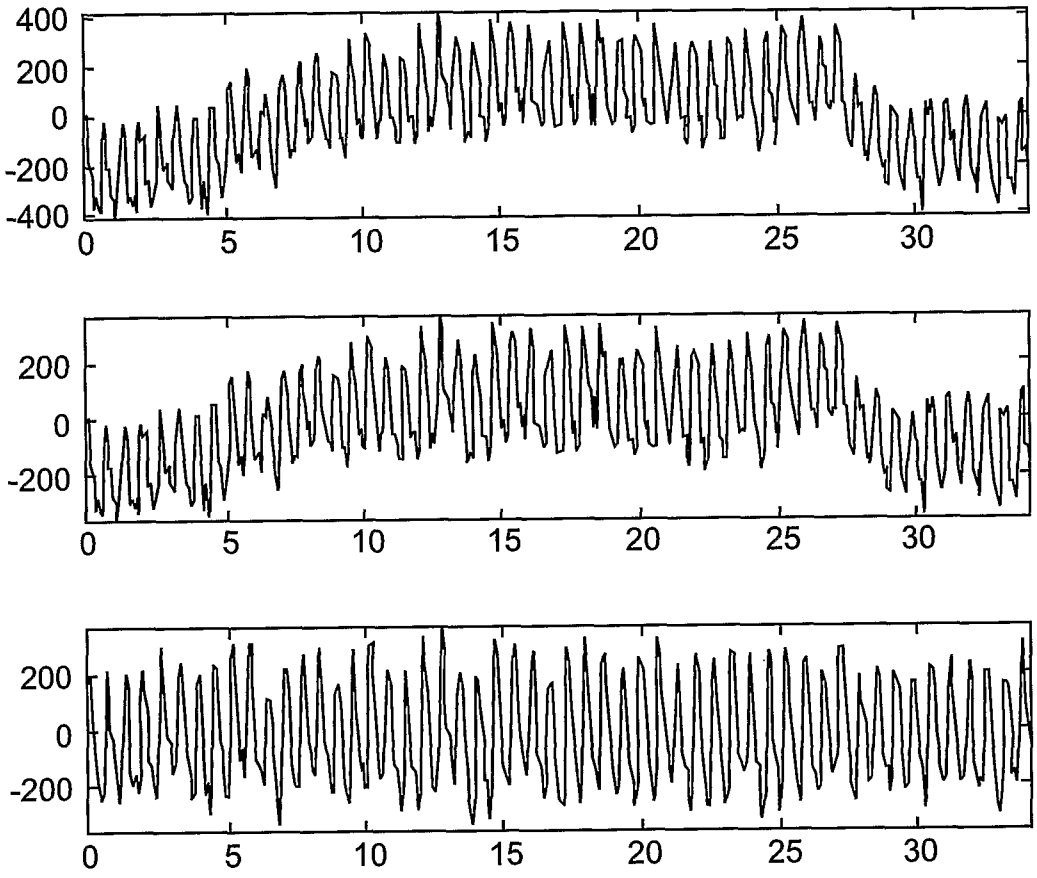
400
200
0
-200
-400
0
5
10
15
20
25
30
200
0
-200
0
5
10
15
20
25
30
200
0
-200
0
5
10
15
20
25
30

Fig. 6e

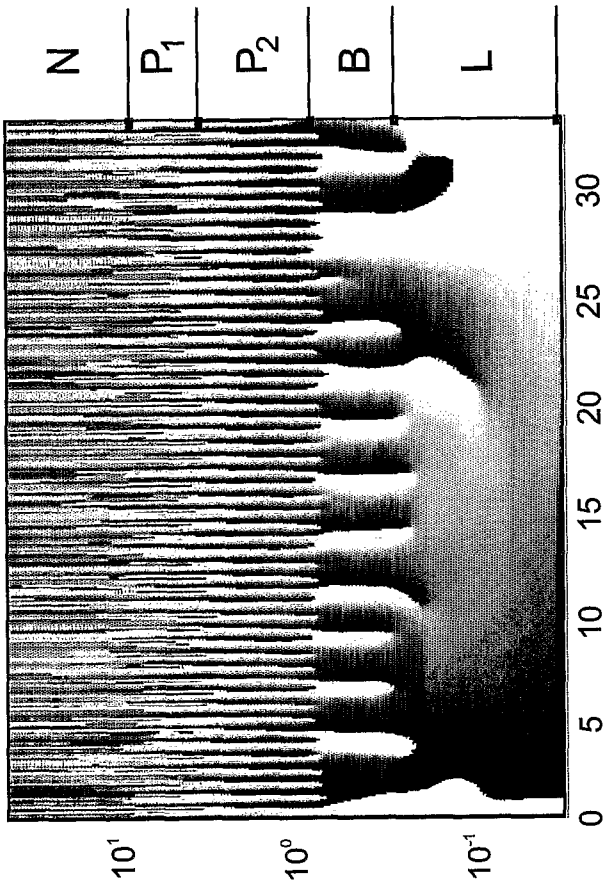

Fig. 7b

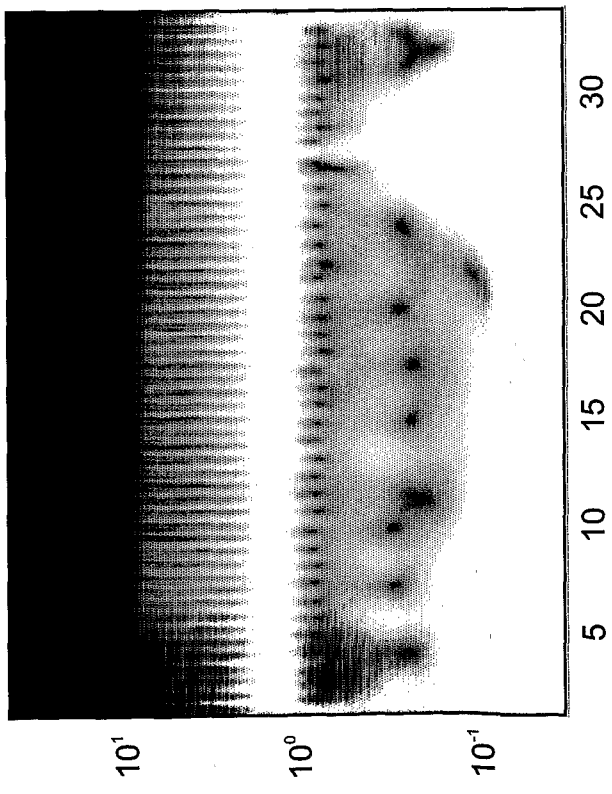

Fig. 7a

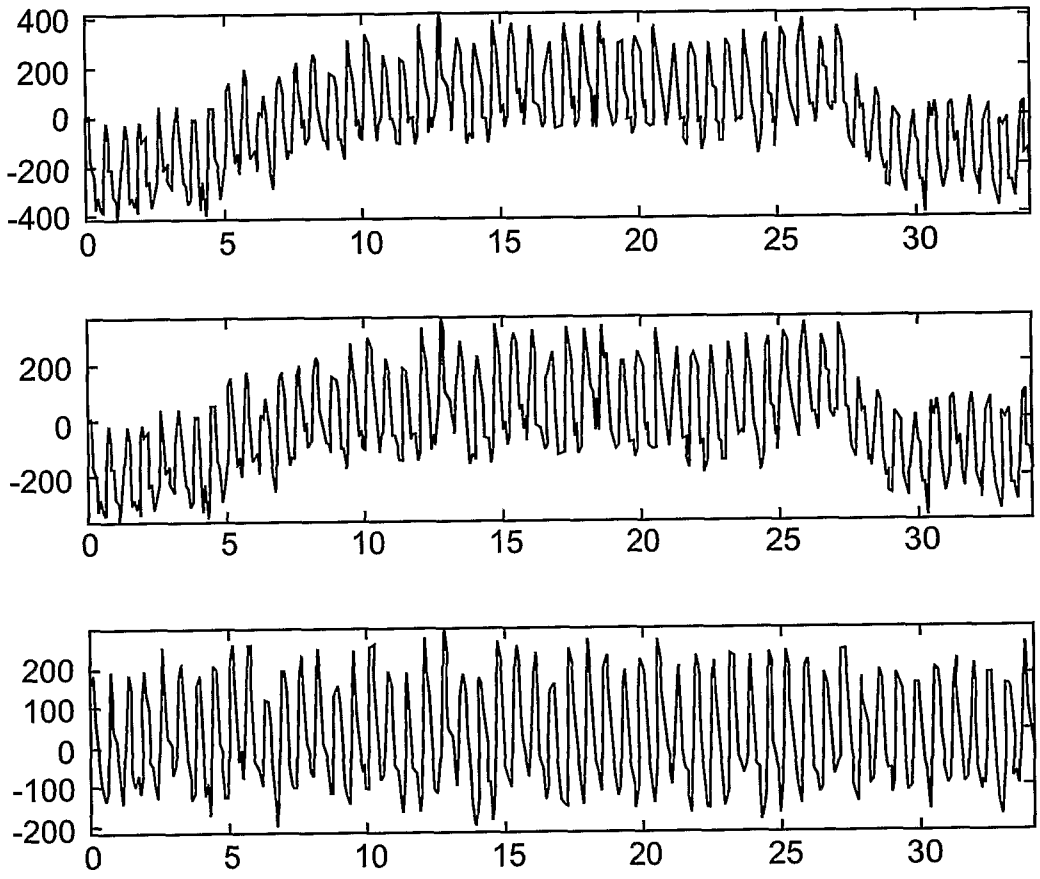
400
200
0
-200
-400
0
5
10
15
20
25
30
200
0
-200
0
5
10
15
20
25
30
200
100
0
-100
-200
0
5
10
15
20
25
30

Fig. 7c

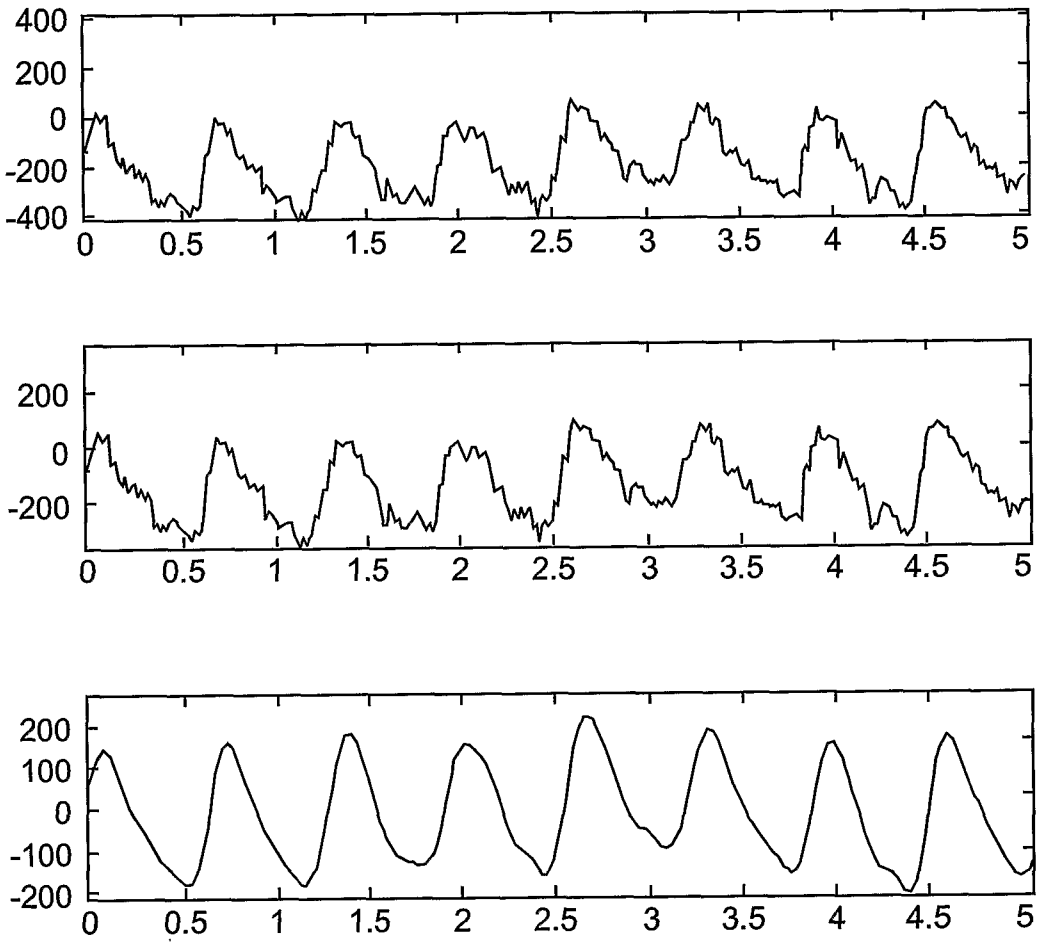
400
200
0
-200
-400
0 0.5 1 1.5 2 2.5 3 3.5 4 4.5 5
200
0
-200
0 0.5 1 1.5 2 2.5 3 3.5 4 4.5 5
200
100
0
-100
-200
0 0.5 1 1.5 2 2.5 3 3.5 4 4.5 5

Fig. 7d

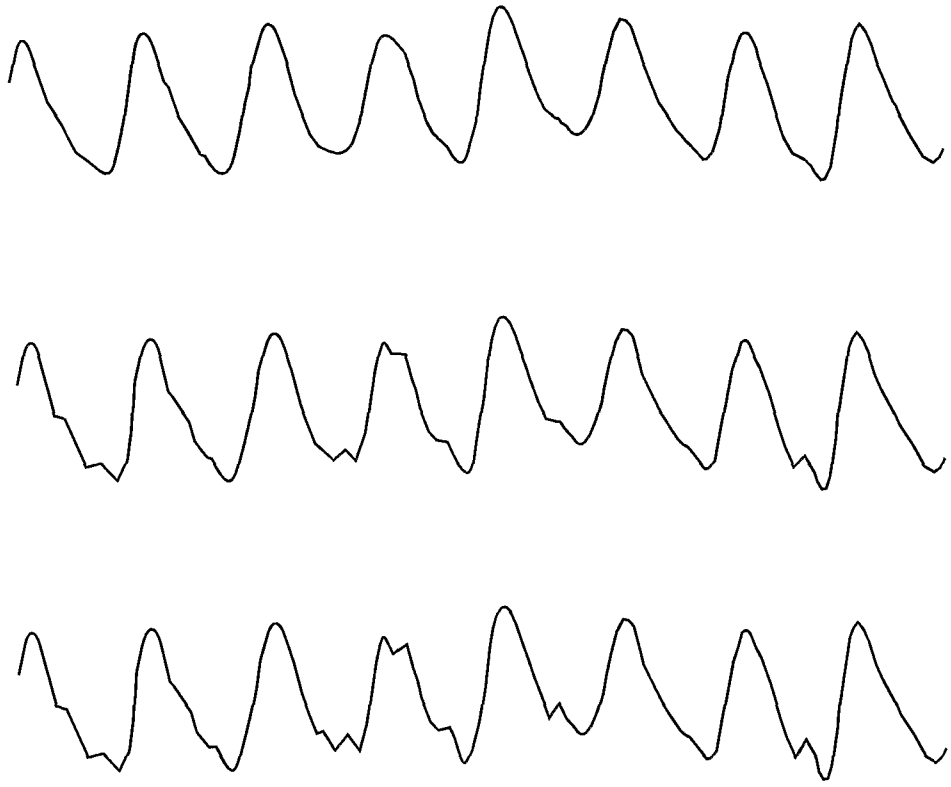

Fig. 7e

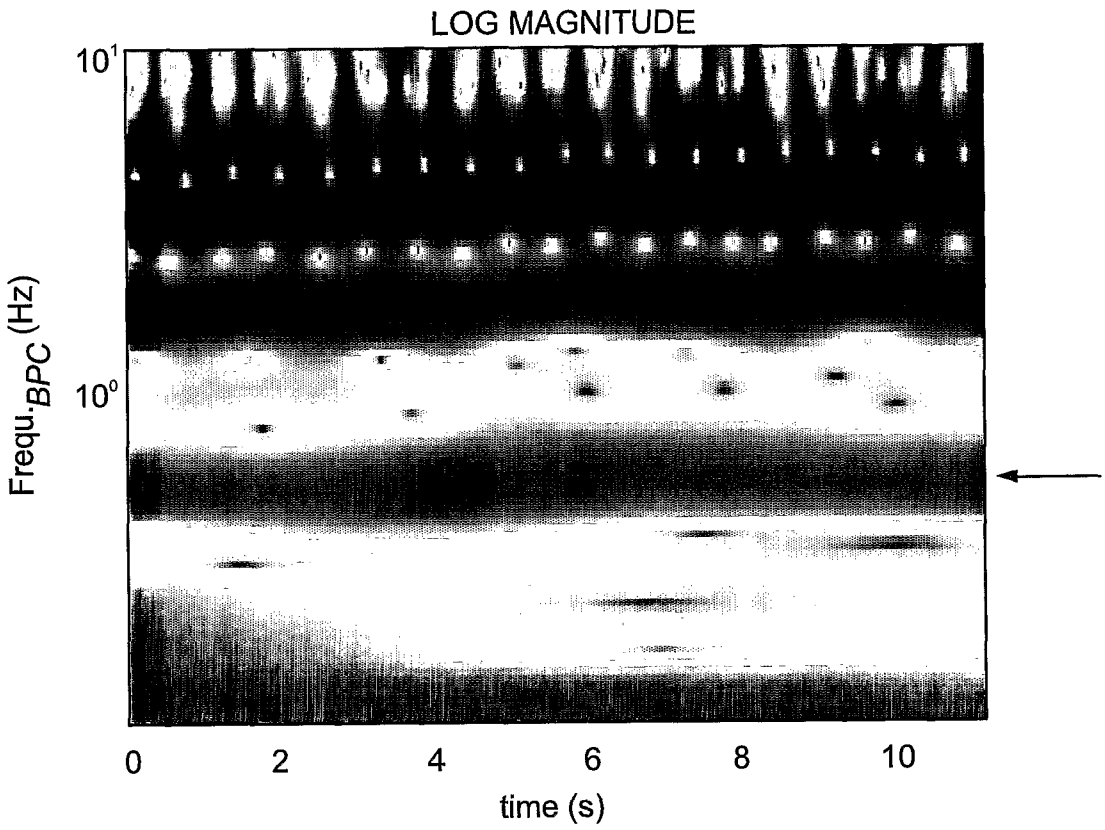
LOG MAGNITUDE
10^1
10^0
Frequ.$_{BPC}$ (Hz)
0
2
4
6
8
10
time (s)

Fig. 8a

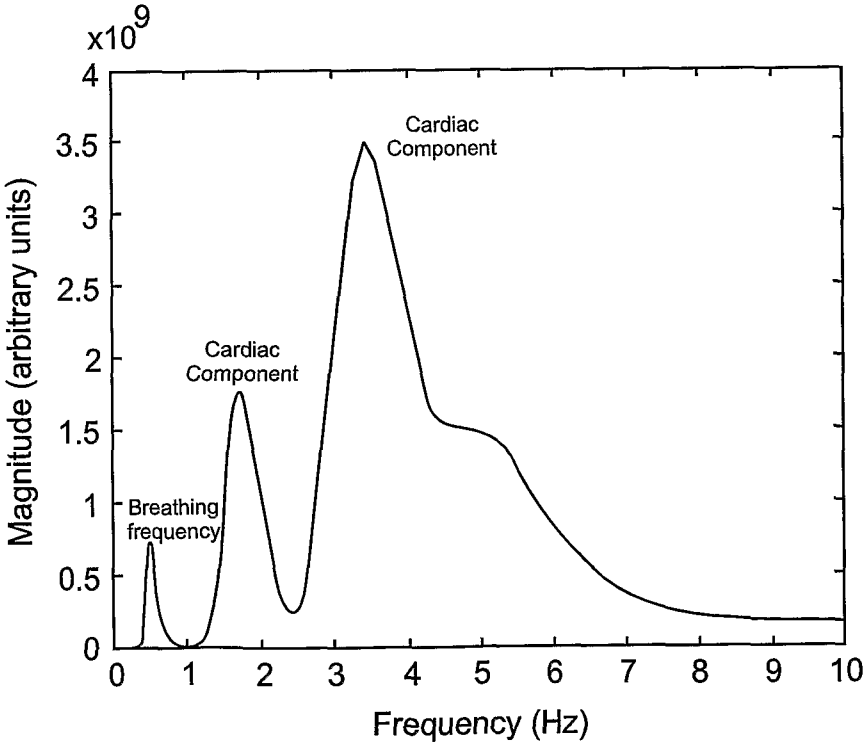
x10^9
4
3.5
3
2.5
2
1.5
1
0.5
0
Magnitude (arbitrary units)
Cardiac Component
Cardiac Component
Breathing frequency
0
1
2
3
4
5
6
7
8
9
10
Frequency (Hz)

Fig. 8b

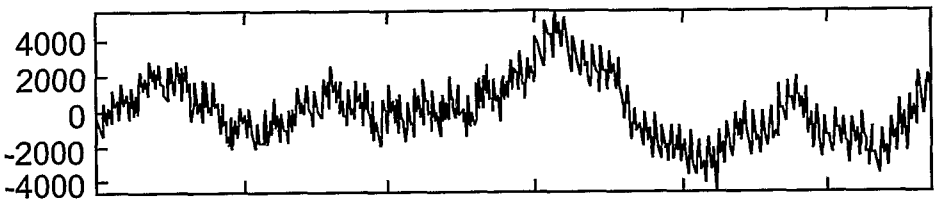

Fig. 9a

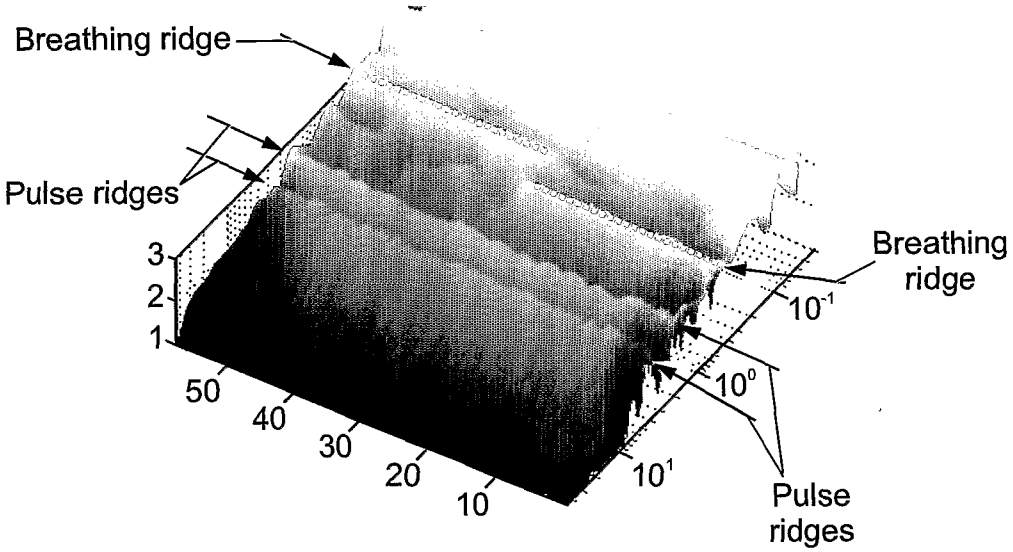

Fig. 9b

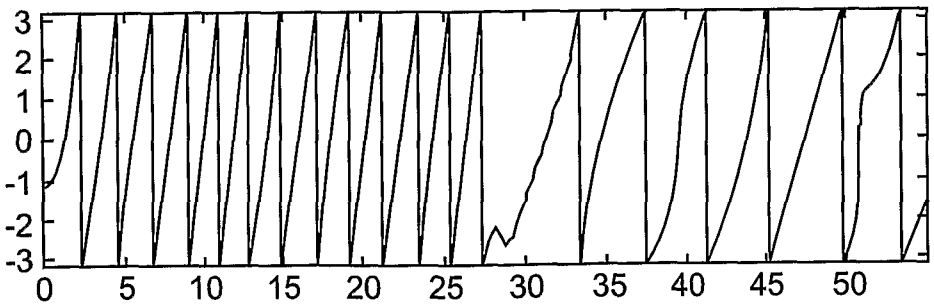

Fig. 9c

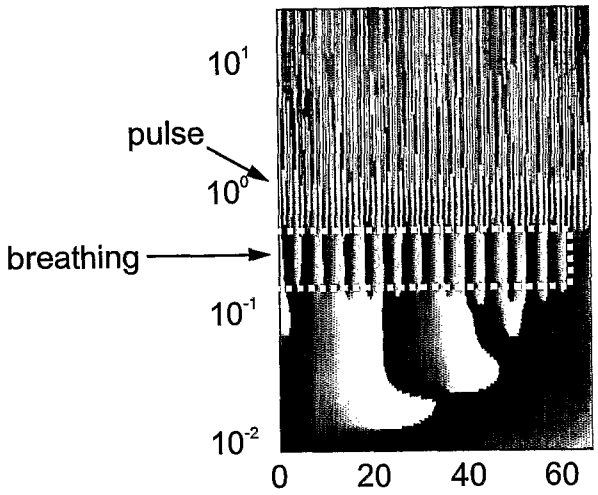

Fig. 10a

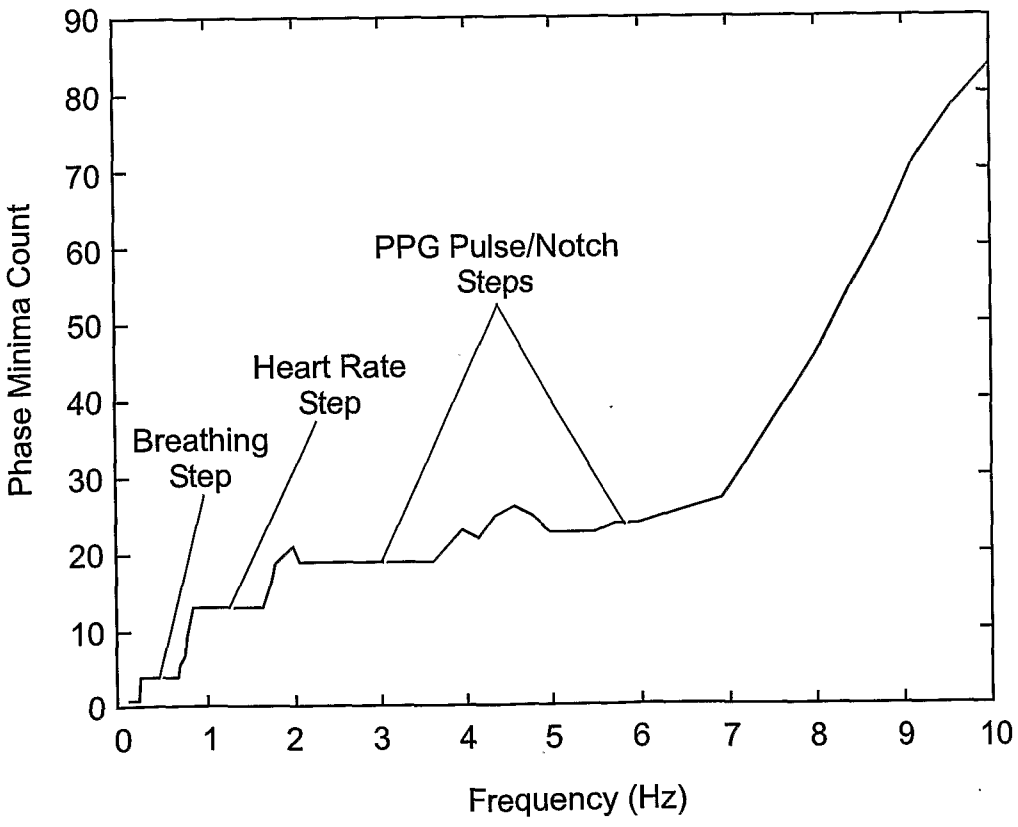

Fig. 10b

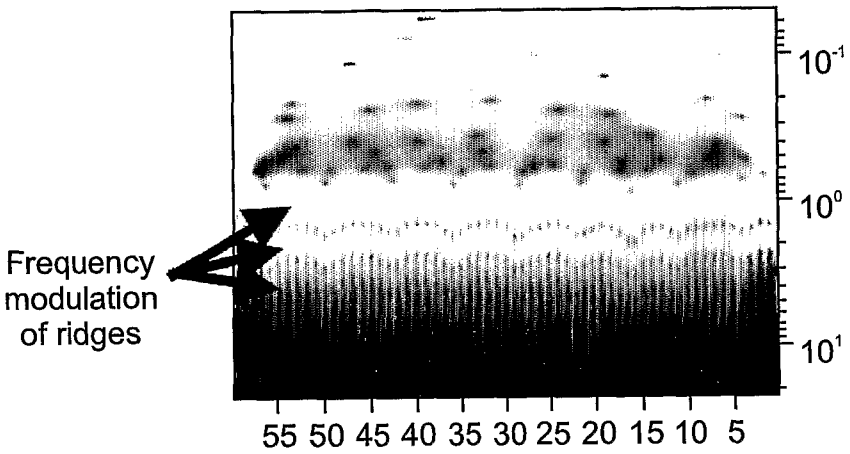

Fig. 11a

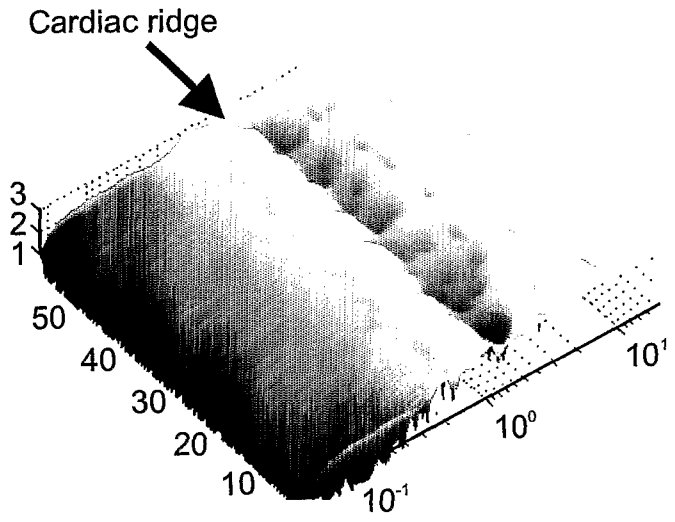

Fig. 11b

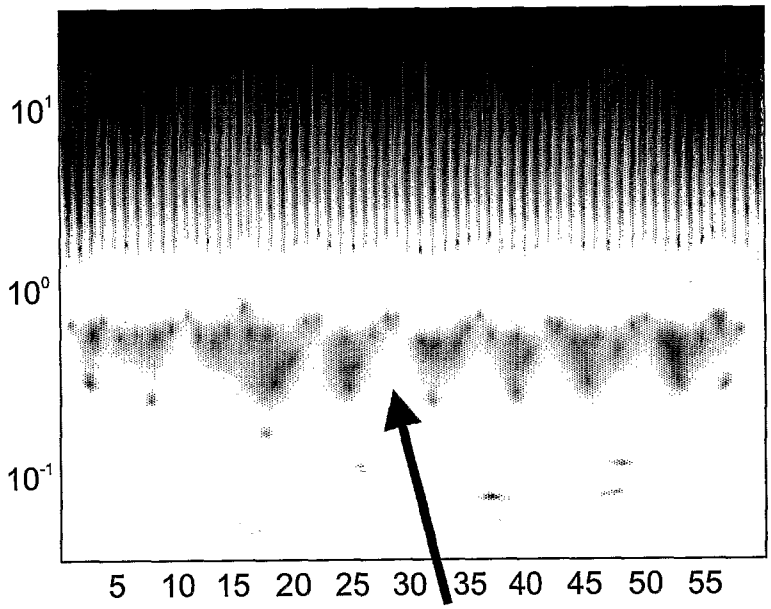

Fig. 11c

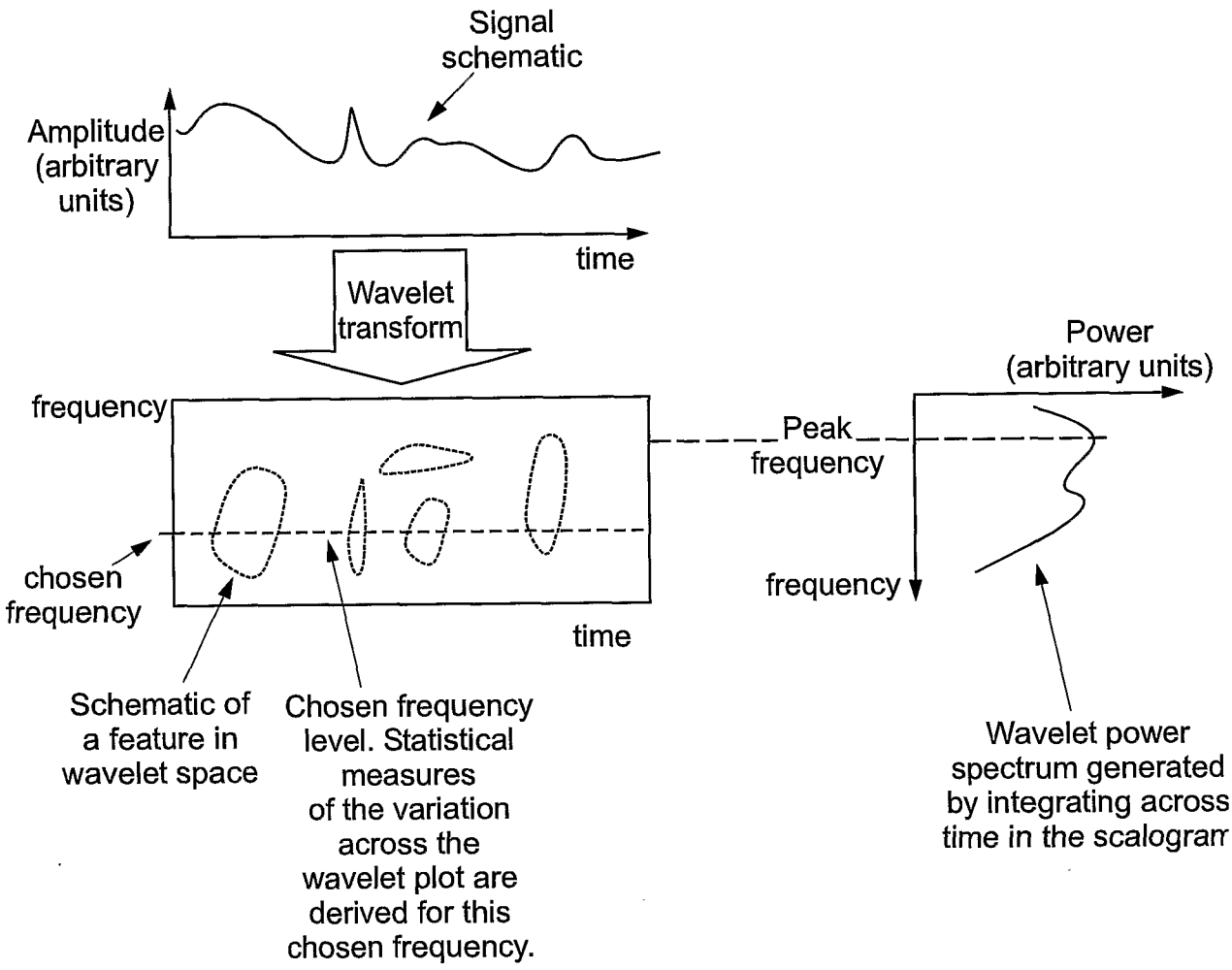
Signal schematic
Amplitude (arbitrary units)
time
Wavelet transform
frequency
chosen frequency
time
Peak frequency
Power (arbitrary units)
frequency
Schematic of a feature in wavelet space
Chosen frequency level. Statistical measures of the variation across the wavelet plot are derived for this chosen frequency.
Wavelet power spectrum generated by integrating across time in the scalogram

Fig. 12

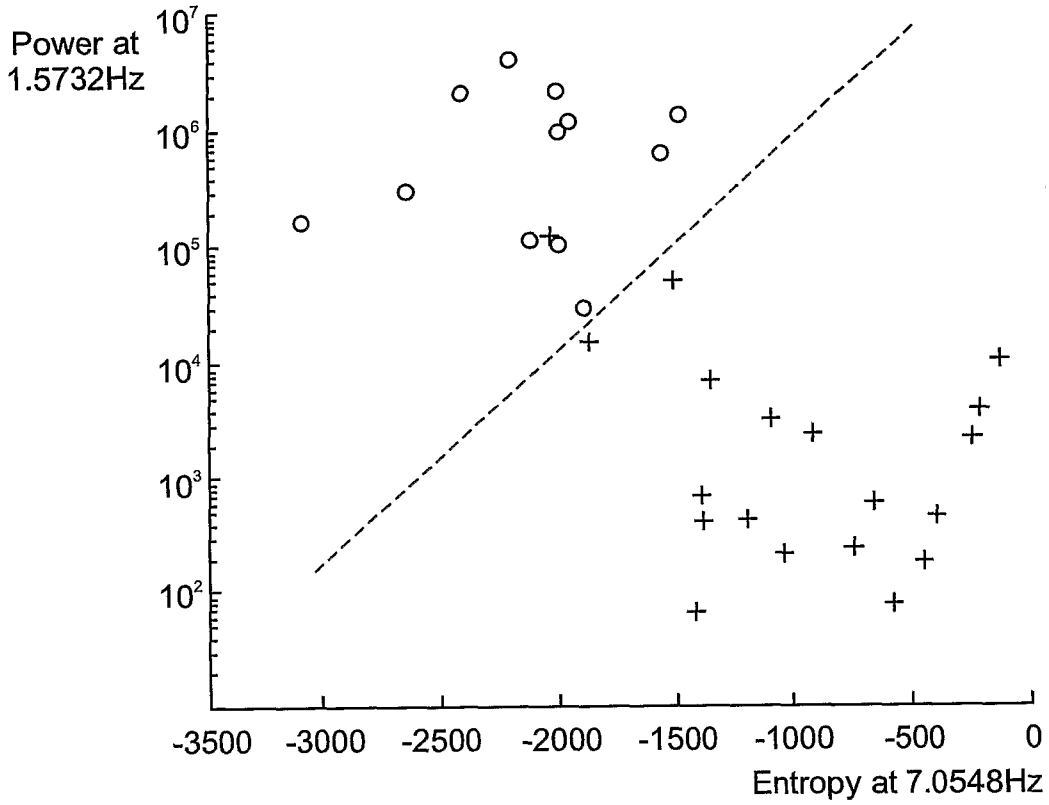

Legend:

'o' - healthy controls.
'+' - children attending the accident and emergency department

Fig. 13

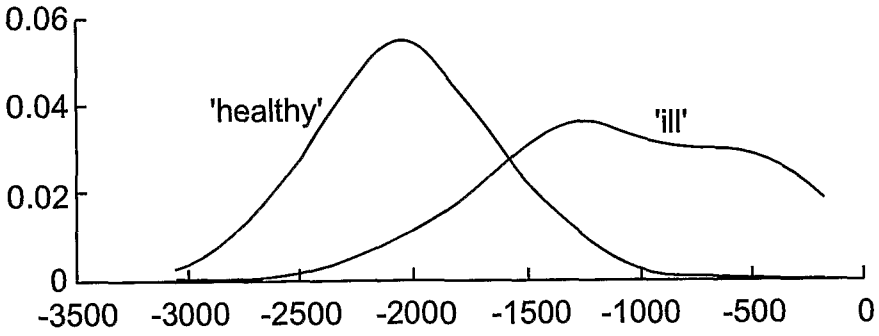

Fig. 14a

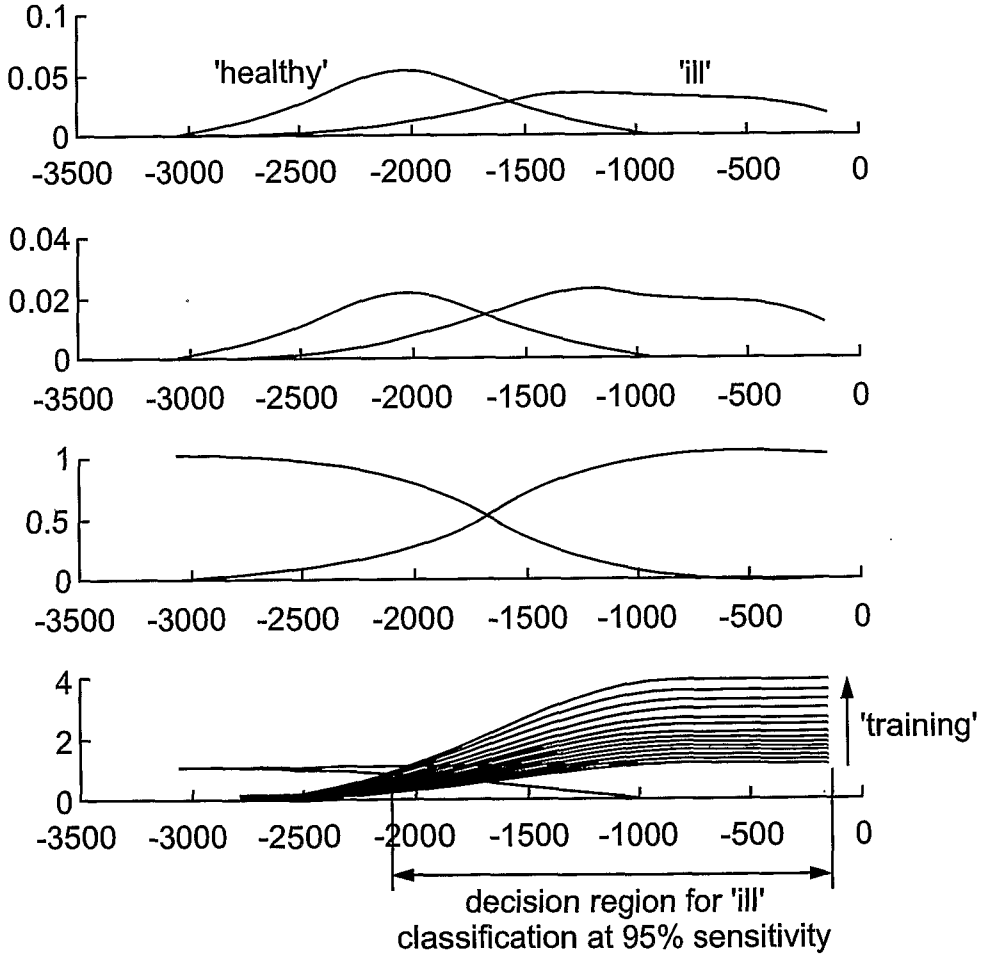

Fig. 14b

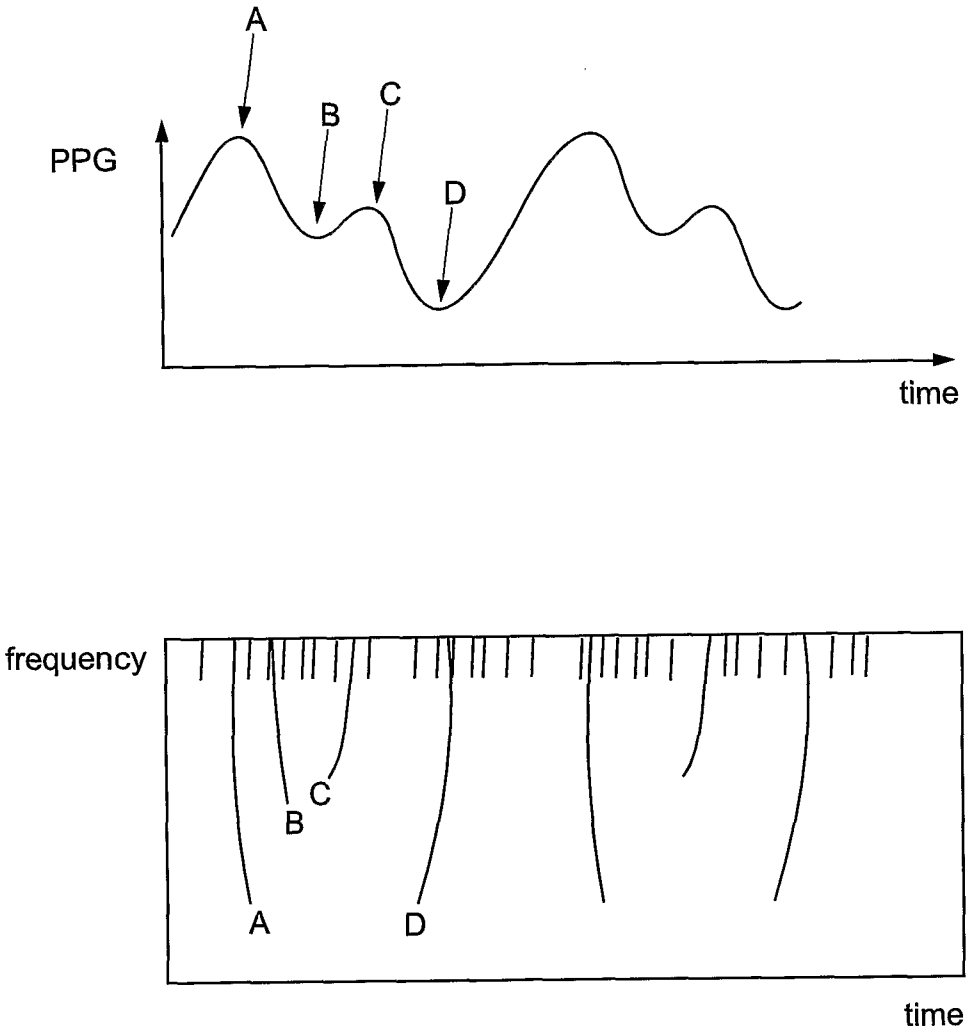

Fig. 15

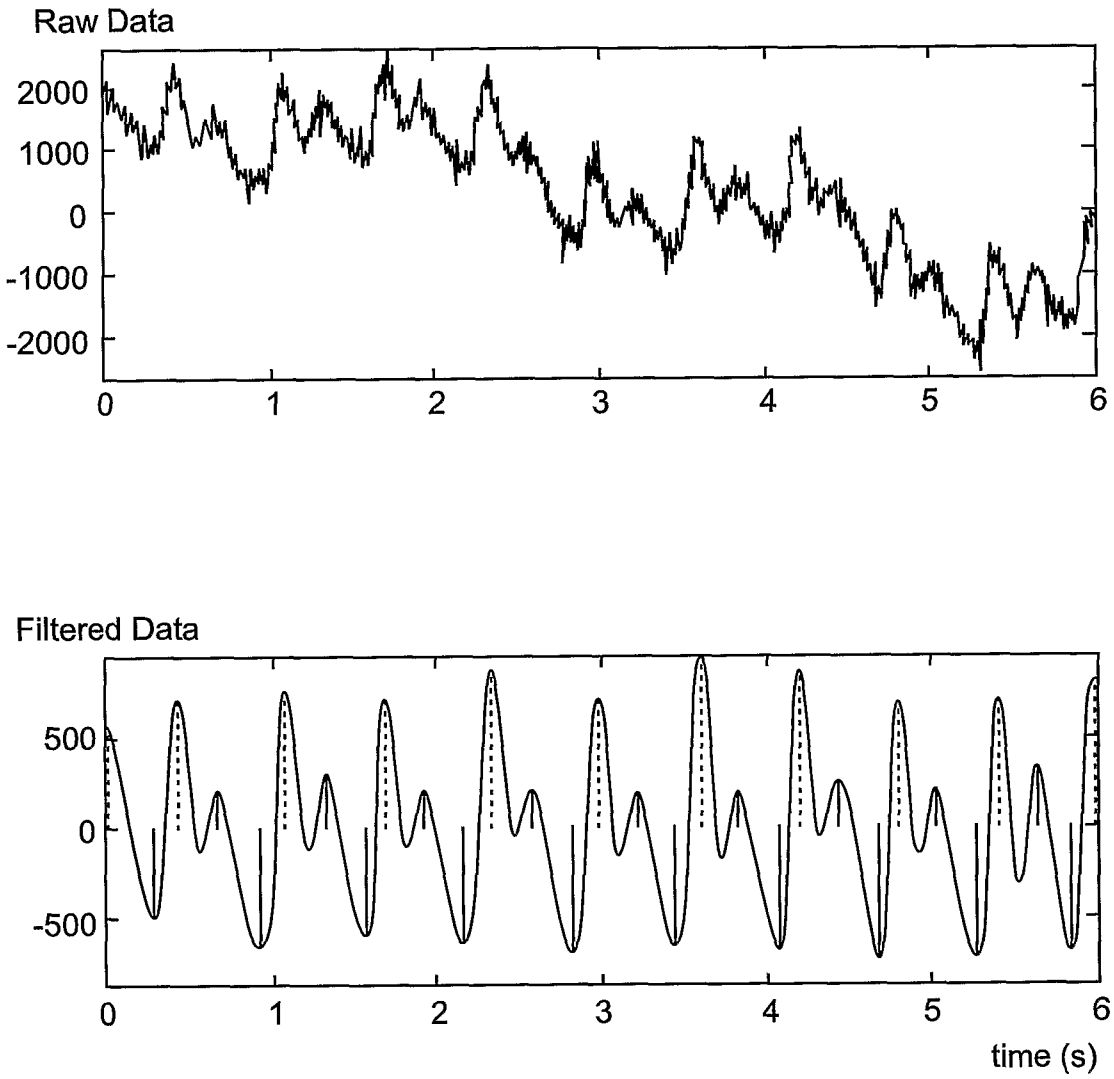
Raw Data
2000
1000
0
-1000
-2000
0
1
2
3
4
5
6
Filtered Data
500
0
-500
0
1
2
3
4
5
6
time (s)

Fig. 16

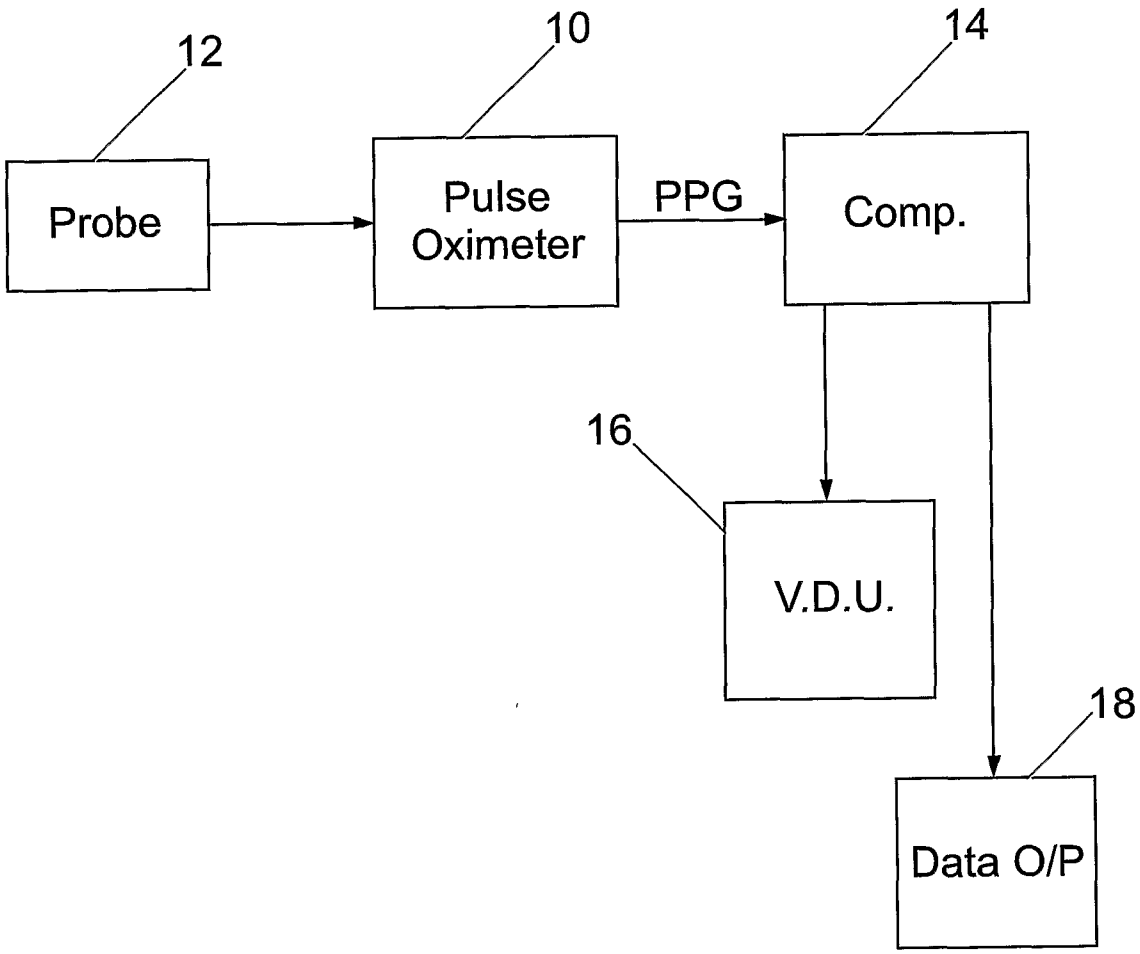

Fig. 17

INTERNATIONAL SEARCH REPORT

Internati Application No
PCT/GB 02/02843

A. CLASSIFICATION OF SUBJECT MATTER
IPC 7 A61B5/00 G06F17/00

According to International Patent Classification (IPC) or to both national classification and IPC

B. FIELDS SEARCHED

Minimum documentation searched (classification system followed by classification symbols)
IPC 7 A61B G06F

Documentation searched other than minimum documentation to the extent that such documents are included in the fields searched

Electronic data base consulted during the international search (name of data base and, where practical, search terms used)

C. DOCUMENTS CONSIDERED TO BE RELEVANT

Category °	Citation of document, with indication, where appropriate, of the relevant passages	Relevant to claim No.
X	WO 01 25802 A (NTC TECHNOLOGY INC) 12 April 2001 (2001-04-12) page 8, line 7 - line 30 page 10, line 17 - line 30 page 12, line 8 -page 13, line 3 page 17, line 30 -page 18, line 16 page 23, line 24 -page 24, line 31 ---	2,3, 8-10,12, 17,22,23
X	US 6 011 985 A (ATHAN STEPHAN PETER ET AL) 4 January 2000 (2000-01-04) column 5, line 48 -column 11, line 39; figure 2A --- -/--	2,3,8,9, 12,22,23

[X] Further documents are listed in the continuation of box C.

[X] Patent family members are listed in annex.

° Special categories of cited documents :

"A" document defining the general state of the art which is not considered to be of particular relevance

"E" earlier document but published on or after the international filing date

"L" document which may throw doubts on priority claim(s) or which is cited to establish the publication date of another citation or other special reason (as specified)

"O" document referring to an oral disclosure, use, exhibition or other means

"P" document published prior to the international filing date but later than the priority date claimed

"T" later document published after the international filing date or priority date and not in conflict with the application but cited to understand the principle or theory underlying the invention

"X" document of particular relevance; the claimed invention cannot be considered novel or cannot be considered to involve an inventive step when the document is taken alone

"Y" document of particular relevance; the claimed invention cannot be considered to involve an inventive step when the document is combined with one or more other such documents, such combination being obvious to a person skilled in the art.

"&" document member of the same patent family

Date of the actual completion of the international search	Date of mailing of the international search report
11 October 2002	21/10/2002

Name and mailing address of the ISA	Authorized officer
European Patent Office, P.B. 5818 Patentlaan 2 NL – 2280 HV Rijswijk Tel. (+31–70) 340–2040, Tx. 31 651 epo nl, Fax: (+31–70) 340–3016	Artikis, T

Form PCT/ISA/210 (second sheet) (July 1992)

INTERNATIONAL SEARCH REPORT

Internat ıpplication No
PCT/GB 02/02843

C.(Continuation) DOCUMENTS CONSIDERED TO BE RELEVANT

Category °	Citation of document, with indication,where appropriate, of the relevant passages	Relevant to claim No.
X	US 6 117 075 A (BARNEA OFER) 12 September 2000 (2000-09-12) column 4, line 38 -column 7, line 20; figure 4	2,3, 8-11, 22-24
A	US 6 208 951 B1 (DIXIT NARENDRA MADHUKAR ET AL) 27 March 2001 (2001-03-27) column 2, line 1 -column 6, line 37 column 7, line 30 -column 9, line 33	2-4, 6-11,17, 18,22-24
A	US 6 135 966 A (KO GARY KAM-YUEN) 24 October 2000 (2000-10-24) abstract; figures 3,8A,8B	2-4, 6-10,12, 22,23
P,A	WO 01 82099 A (WATSON JAMES NICHOLAS ;ADDISON PAUL STANLEY (GB); COURT OF NAPIER) 1 November 2001 (2001-11-01) the whole document	1-24

INTERNATIONAL SEARCH REPORT

Inte nal application No.
PCT/GB 02/02843

Box I Observations where certain claims were found unsearchable (Continuation of item 1 of first sheet)

This International Search Report has not been established in respect of certain claims under Article 17(2)(a) for the following reasons:

1. [X] Claims Nos.: 1 and its dependent claims
because they relate to subject matter not required to be searched by this Authority, namely:

Rule 39.1(iv) PCT - Diagnostic method practised on the human or animal body.
Claim 2 and all claims dependent on it (except claim 21) have been searched.

2. [ ] Claims Nos.:
because they relate to parts of the International Application that do not comply with the prescribed requirements to such an extent that no meaningful International Search can be carried out, specifically:

3. [ ] Claims Nos.:
because they are dependent claims and are not drafted in accordance with the second and third sentences of Rule 6.4(a).

Box II Observations where unity of invention is lacking (Continuation of item 2 of first sheet)

This International Searching Authority found multiple inventions in this international application, as follows:

1. [ ] As all required additional search fees were timely paid by the applicant, this International Search Report covers all searchable claims.

2. [ ] As all searchable claims could be searched without effort justifying an additional fee, this Authority did not invite payment of any additional fee.

3. [ ] As only some of the required additional search fees were timely paid by the applicant, this International Search Report covers only those claims for which fees were paid, specifically claims Nos.:

4. [ ] No required additional search fees were timely paid by the applicant. Consequently, this International Search Report is restricted to the invention first mentioned in the claims; it is covered by claims Nos.:

Remark on Protest

[ ] The additional search fees were accompanied by the applicant's protest.

[ ] No protest accompanied the payment of additional search fees.

INTERNATIONAL SEARCH REPORT

Information on patent family members

Internat Application No
PCT/GB 02/02843

Patent document cited in search report	Publication date	Patent family member(s)	Publication date
WO 0125802 A	12-04-2001	US 6393311 B1	21-05-2002
		EP 1224566 A2	24-07-2002
		EP 1121051 A2	08-08-2001
		WO 0125802 A2	12-04-2001
		WO 0022408 A2	20-04-2000
US 6011985 A	04-01-2000	US 5575284 A	19-11-1996
US 6117075 A	12-09-2000	AU 5706299 A	10-04-2000
		EP 1123038 A1	16-08-2001
		JP 2002528146 T	03-09-2002
		WO 0016687 A1	30-03-2000
US 6208951 B1	27-03-2001	NONE	
US 6135966 A	24-10-2000	AU 3695799 A	23-11-1999
		CA 2330572 A1	11-11-1999
		WO 9957647 A1	11-11-1999
		CN 1299486 T	13-06-2001
		EP 1075678 A1	14-02-2001
WO 0182099 A	01-11-2001	AU 4422800 A	07-11-2001
		EP 1173813 A1	23-01-2002
		WO 0182099 A1	01-11-2001

专利名称(译)	基于小波的脉搏血氧饱和度信号分析		
公开(公告)号	EP1399056A1	公开(公告)日	2004-03-24
申请号	EP2002735636	申请日	2002-06-21
[标]申请(专利权)人(译)	CARDIODIGITAL		
申请(专利权)人(译)	CARDIODIGITAL有限公司		
当前申请(专利权)人(译)	NELLCOR PURITAN BENNETT爱尔兰		
[标]发明人	ADDISON PAUL STANLEY WATSON JAMES NICHOLAS		
发明人	ADDISON, PAUL, STANLEY WATSON, JAMES NICHOLAS		
IPC分类号	A61B5/0245 A61B5/00 A61B5/0205 A61B5/08 A61B5/145 G06F17/00 G06K9/00		
CPC分类号	G06K9/00496 A61B5/0205 A61B5/14551 A61B5/6816 A61B5/6826 A61B5/6838 A61B5/7207 A61B5/726 A61B5/7264 A61B5/742		
代理机构(译)	COOPER，JOHN		
优先权	2002006382 2002-03-19 GB 2001015284 2001-06-22 GB		
其他公开文献	EP1399056B1		
外部链接	Espacenet		

摘要(译)

通过小波变换技术分解脉搏血氧饱和度信号，合适地是光电容积描记图（PPG），并且分析分解的信号以提供所选择的生理数据。可以处理信号以去除噪声，伪像或瞬态特征。呼吸信息也可以恢复。